AD-783 274

BURIED ANTENNA PERFORMANCE: DEVELOPMENT OF SMALL RESONANT BURIED ANTENNAS

Howard E. Bussey, et al

National Bureau of Standards

Prepared for:

Rome Air Development Center

June 1974

DISTRIBUTED BY:

NTIS

National Technical Information Service
U. S. DEPARTMENT OF COMMERCE
5285 Port Royal Road, Springfield Va. 22151

UNCLASSIFIED

SECURITY CLASSIFICATION OF THIS PAGE (When Data Entered)

AD-783274

REPORT DOCUMENTATION PAGE		READ INSTRUCTIONS BEFORE COMPLETING FORM
1. REPORT NUMBER RADC-TR-74-169	2. GOVT ACCESSION NO.	3. RECIPIENT'S CATALOG NUMBER
4. TITLE (and Subtitle) BURIED ANTENNA PERFORMANCE; DEVELOPMENT OF SMALL RESONANT BURIED ANTENNAS		5. TYPE OF REPORT & PERIOD COVERED Final Report May 72 - Aug 73
		6. PERFORMING ORG. REPORT NUMBER Project 2727438
7. AUTHOR(s) Howard E. Bussey Ezra B. Larsen		8. CONTRACT OR GRANT NUMBER(s) F30602-72-F-0332
9. PERFORMING ORGANIZATION NAME AND ADDRESS National Bureau of Standards Electromagnetics Division Boulder, Colorado 80302		10. PROGRAM ELEMENT, PROJECT, TASK AREA & WORK UNIT NUMBERS JO 692B0304
11. CONTROLLING OFFICE NAME AND ADDRESS Rome Air Development Center (DCCR) Griffiss Air Force Base, New York 13441		12. REPORT DATE June 1974
		13. NUMBER OF PAGES 104
14. MONITORING AGENCY NAME & ADDRESS (if different from Controlling Office) Same		15. SECURITY CLASS. (of this report) Unclassified
		15a. DECLASSIFICATION/DOWNGRADING SCHEDULE N/A

16. DISTRIBUTION STATEMENT (of this Report)

Approved for public release. Distribution unlimited.

17. DISTRIBUTION STATEMENT (of the abstract entered in Block 20, if different from Report)

Same

18. SUPPLEMENTARY NOTES

None

19. KEY WORDS (Continue on reverse side if necessary and identify by block number)

Antenna Efficiency
Buried Antennas
Depth Attenuation Interface Loss
Resonant Antennas

Reproduced by
NATIONAL TECHNICAL
INFORMATION SERVICE
U S Department of Commerce
Springfield VA 22161

20. ABSTRACT (Continue on reverse side if necessary and identify by block number)

Small resonant dipole antennas at 145 MHz were developed suitable to be buried for concealment. Theory of the pattern and the loss of buried dipoles is summarized. Experiments are described that confirm the theory. The circuit representation of a resonator is utilized in measuring and analyzing the Q, bandwidth, and impedance of the antennas. The field strength performance of buried candidate antennas was measured and agreed with expected losses due to burial and inefficiency. Theoretically a resonant horizontal magnetic

DD FORM 1 JAN 73 1473 EDITION OF 1 NOV 65 IS OBSOLETE

UNCLASSIFIED

SECURITY CLASSIFICATION OF THIS PAGE (When Data Entered)

20. ABSTRACT (continued)

dipole has the lowest burial loss for the fully buried condition. A resonant horizontal electric dipole may have equally low loss in practice because its efficiency is better (for the size allowed). Low (ten centimeter) profile vertical electric dipoles, not fully buried, exhibit even smaller losses and would be useful. The performance of these buried antennas could be improved by allowing a larger encapsulation.

FOREWORD

This Final Report is by the National Bureau of Standards, Electromagnetics Division, Boulder, Colorado, for Rome Air Development Center, Griffiss Air Force Base, New York, under Contract F30602-72-F-0332, Job Order 692B0304. NBS Project Number is 2727438. Mr. Russell A. King (DCCN) was the RADC Project Engineer.

The report describes a study performed from May 1972 to August 1973.

The authors acknowledge the helpful advice and contributions as readers of R.C. Baird, C.F. Stuben Rauch, and R.G. Fitsgerrel. G.A. Hufford gave helpful explanations. M.L. Crawford and A.C. Wilson gave information on antennas and with J.E. Chukoski aided with calibration and field measurements.

This report has been reviewed by the RADC Information Office (OI) and is releasable to the National Technical Information Service (NTIS).

This technical report has been reviewed and is approved.

APPROVED:

RUSSELL A. KING
Project Engineer

APPROVED:

FRED I. DIAMOND, Technical Director
Communications and Navigation Division

FOR THE COMMANDER:

JOHN P. HUSS
Acting Chief, Plans Office

Evaluation

This effort was a study to investigate, theoretically and experimentally, the possibility of Burst Communication by radio transmission from an antenna buried for concealment. Low transmitter power, 1 watt, maximum antenna width of 5 inches and VHF frequency were major parameters. The emphasis was on antenna design and not communications system design. The results of the study indicate theoretically useful ground to airborne communications.

In view of the theoretical and experimental feasibility indicated, an expansion of the effort is recommended. It should include further experimentation and flight testing to explore the more practical aspects of adapting the experimental antennas to existing buried transmit devices. An experimental buried antenna/transmit combination unit should be constructed for this purpose.

Laurella King

TABLE OF CONTENTS

Section	Title	Page
1.	INTRODUCTION	1
2.	THEORETICAL FIELD CALCULATIONS	2
	A. Introduction	2
	B. Gain Pattern in Air of a Buried Dipole	2
	C. Theoretical Derivation of Pattern Gain	6
	D. Physical Optics of Buried Antennas	8
	E. Ground Wave	10
	F. Calculation of Field From Equations (1)	11
	G. Efficiency	17
3.	EXPERIMENTS COMPARED TO EQUATIONS (1)	18
	A. Introduction	18
	B. Transmitted Power	18
	C. Field Strength Calibration	22
	D. Comparison of Theory and Experiment for a "Reference" Monopole	23
	E. Far Field Pattern Versus Elevation Angle	25
	F. Measured Loss of Rather Ideal Buried Dipoles	25
	G. Effect of Shallow Burial	30
	H. Summary	32
4.	DEVELOPMENT OF MINIATURE RESONANT ANTENNAS	34
	A. Introduction	34
	B. Construction Details	34
	C. Impedance Measurements with the Network Analyzer	42
	D. Circuit Representation and Q Analysis	43
	E. Antenna Efficiency	46
	F. Coupling Coefficients, Theory, and Experiments for One Antenna	51
	G. Coupling, and Radiation Resistance Discussion of All Antennas	56
	H. Interaction with Burial Medium	61

TABLE OF CONTENTS (Concluded)

Section	Title	Page
	I. Bandwidth Improvement	62
	J. Additional Modification of Antennas; Resulting Bandwidth and Interaction with Media	64
	K. Conclusions for Section 4	67
5.	FIELD TESTS OF BURIED ANTENNAS	69
	A. Introduction	69
	B. Theoretical and Practical Considerations	69
	C. Field Site Performance of Small Antennas	70
	D. Summary of Resonant Antennas	76
6.	PREDICTED DISTANCE OF COMMUNICATION	77
	A. Introduction	77
	B. Assumed Transmitter Power and Receiver Characteristics	77
	C. Gain Pattern Over a Spherical Earth	78
	D. Field Strength Versus Distance	78
7.	DISCUSSION AND CONCLUSIONS	81
	ACKNOWLEDGMENTS	84
	REFERENCES	85
	BIBLIOGRAPHY ON BURIED ANTENNAS	87

LIST OF ILLUSTRATIONS

Figure	Title	Page
1.	(a) The ray at critical angle θ_c becomes horizontal after refraction. Rays outside of the cone θ_c suffer total internal reflection. (b) Illustrating the divergence of the refraction from a buried point source.	5
2.	Interface and pattern loss of the TM wave, E_θ wave, of a buried horizontal magnetic dipole (depth attenuation omitted). The TM wave (end fire) from a buried HED has this loss plus the small additional end fire pattern loss shown in figure 4.	13
3.	Depth attenuation, dB, at 145 MHz versus ε' with conductivity, σ, S/m, as a parameter. The ordinate is nearly linear in S except at low ε'. Elevation angle is 2°, but results are accurate for the range of 1 to 10° to within approximately 0.01 dB.	14
4.	Loss due to the underground pattern factor for the end fire direction from a buried horizontal dipole, and for a buried vertical dipole. The elevation angle of the field point in the air is 1°; however, at any angle below 10° elevation the results are accurate to 0.1 dB.	15
5.	Interface and pattern loss of the TE wave, E_ϕ wave, of buried horizontal electric dipole (HED) broadside (depth attenuation omitted). The TE wave (end fire) from a buried HMD has this loss plus the small additional end fire loss shown in figure 4.	16
6.	(a) Equipment arrangement for measuring gain pattern of buried antenna. (b) Showing the main measurement parameters, frequency, forward and reverse powers, and cable lengths u and u_r which contribute attenuation. The attenuation due to u_r was included as an integral part of the FIM sensitivity calibration.	19
7.	Attenuation of the transmitting RG-9B cable versus frequency at 32° and 72°F, and an interpolated curve at 50°F.	20

LIST OF ILLUSTRATIONS (Continued)

Figure	Title	Page
8.	Field strength conversion factor for Field Intensity Meter (FIM), as measured by NBS standard field method. The factor in dB is added to the voltmeter indication to give the electric field in the air.	21
9.	Theoretical far field power gain pattern of reference monopole (quarter wavelength whip on a one wavelength diameter ground plane set on the earth's surface).	26
10.	Measured field strength in dB > 1 μV/m at R = 30.5 m distance of sleeved dipole and reference monopole at 145 MHz. Antenna power, P_a of equation (21), is 1 W; $\varepsilon' \sim 10$; $\sigma \sim 0.06$ S/m.	28
11.	Measured field strength in dB > 1 μV/m at R = 30.5 m distance, of a folded dipole, F = 300 MHz. Antenna power, P_a of equation (21), is 1 W; $\varepsilon' \sim 10$; conductivity ~ 0.06 S/m.	29
12.	Measured field strength in dB > 1 μV/m at R = 30.5 m, F = 300 MHz, P_a = 1 W, from antenna A3, which is a miniature vertical electric dipole, VED, measured as a function of antenna height.	31
13.	Antenna A8, a coil and a capacitor excited as an asymmetric vertical dipole. Also may be referred to as a monopole on a base plate.	35
14.	Antenna C4, a resonant helix partially imaged by the base.	36
15.	Antenna B3, HED formed by a resonant coil and capacitor.	37
16.	Antenna B4, HED formed by coil and capacitor.	38
17.	Antenna D3, HMD, a loop approximately 10 cm square resonated by a capacitor, C = 6 pF.	39
18.	Antenna D4, horizontal coil, probably much overcoupled; see section 4F for coupling adjustment.	40

LIST OF ILLUSTRATIONS (Continued)

Figure	Title	Page
19.	Antenna D5, self resonant helix with diameter and pitch to make HMD equal to HED.	41
20.	Lumped circuit representation of a resonator terminating a transmission line. (a) Represents a series resonant circuit. (b) Transforms to (c), a parallel resonant circuit, which agrees with experiment.	44
21.	Impedance plot and Q analysis of impedance points measured at 0.2 MHz intervals, in the rectangular impedance plane for antenna D3 (10 cm diameter loop) enclosed in a copper cavity (radiansphere). Points are fitted by a circle.	47
22.	Plot and Q analysis as in figure 21 except that the antenna D3 is radiating into an anechoic chamber.	48
23.	Impedance plot for antenna model D3-2 with length of coupling link d = 6.7 cm.	54
24.	Impedance plot for model D3-4, d = 4.5 cm.	54
25.	Impedance plot for model D3-6, d = 2.5 cm.	55
26.	Impedance plot for model D3-8, with coupling d = 4.5 cm as in D3-4, and firmly soldered in place.	55
27.	Impedance plot for model D3-8, buried in concrete, permittivity ∿ 6.5, loss tangent ∿ 0.01.	57
28.	Impedance plot for antenna A8 in anechoic room.	57
29.	Impedance plot for antenna C4 in anechoic room.	58
30.	Impedance plot for antenna B3 in anechoic room.	58
31.	Impedance plot for antenna B4 in anechoic room.	59
32.	Impedance plot for antenna D3 in anechoic room.	59
33.	Impedance plot for antenna D5 in anechoic room.	60
34.	Circuit used for analyzing change of resonant frequency due to burial.	60

LIST OF ILLUSTRATIONS (Concluded)

Figure	Title	Page
35.	Field strength versus elevation angle of various buried antennas, and the unburied reference monopole, normalized to 1 W power accepted by the antenna. Burial is in concrete, $\varepsilon' \sim 6.5$. Range distance is 30.5 m. Estimated ground constants are $\varepsilon' = 12$, $\sigma = 0.05$ S/m.	71
36.	Field strength versus elevation angle of modified antennas; as in figure 35, burial is in concrete. Ground is drier, estimate $\varepsilon' = 7$, $\sigma = 0.03$ S/m. Antennas A8 and C4 are at the interface, partially buried.	74
37.	Electric field strength, dBV/m, from various antennas accepting 1 W power. The curves marked HMD are for a buried horizontal magnetic dipole. Curve M is for a low profile VED with efficiency = 0.4. E_f is the free space field of an isotropic source.	79

LIST OF TABLES

Table	Short Title	Page
1.	Power gains of various antennas.	4
2.	Theoretical and measured fields of "reference" monopole.	24
3.	Comparison of low-angle losses of "reference" monopole and buried antennas with interface loss only.	27
4.	Measured Q, resistance, and efficiency of antennas.	50
5.	Theoretically estimated resistances and efficiencies of antennas.	52
6.	Change of resonant frequency due to burial.	63
7.	Measured bandwidths of antennas.	65
8.	Characteristics of changed antennas.	66
9.	Conversion factor to obtain field strength from voltage measured by FIM.	73

1. INTRODUCTION

The objective of this effort is to provide engineering services to study the feasibility and practicality of low power radio frequency transmissions from antennas that are buried just below the surface of the earth. Burial is for concealment only.

The main purpose is to predict the communications range to an assumed receiver from a buried transmitting antenna. In doing this the theory of buried antennas, which is available in the literature, is outlined; experiments were performed to confirm the theory; and small resonant antennas for burial were developed and tested. Construction details are given for some candidate antennas.

Compromises and trade-offs are described for various types of antennas, e.g., vertical and horizontal dipoles. The main factor in the research is the requirement of a small antenna to allow convenient burial deployment. This requirement was accomplished by the use of resonant antennas at the assigned frequency, 145 MHz.

The theory of emission from a buried source to the air space is discussed in section 2. The general properties of resonant antennas are described in section 3. The effects of burial on impedance, bandwidth, efficiency, and pattern are described in section 4, and a series of candidate antennas is described. Experimental results for the candidates are given in section 5. The maximum communication range is predicted in section 6.

2. THEORETICAL FIELD CALCULATIONS

A. INTRODUCTION

A theoretical discussion of the effect of burial in the ground on antenna performance consists of three main aspects: one aspect is the change of the efficiency of the antenna; the second aspect is the exact field pattern calculation; and the third aspect is the change in impedance, and especially the change in the resonant frequency of resonant antennas. The determination of efficiency of buried antennas by theoretical methods has been done only for certain antennas, e.g., for a spherical dipole [1]. Theoretical work on efficiency was not done in the present contract. Experimental determinations of efficiency are discussed in a later section.

The field at a receiving point in the air may be compared to that from a monopole set on the ground at the place where the radiation emerges from the buried antenna. This method makes it clear how much loss arises from the burial. A more rigorous method is to state the loss relative to an isotropic source. This method shows the total effect of the burial and the propagation. Both presentations will be used.

B. GAIN PATTERN IN AIR OF A BURIED DIPOLE

The field in the air space is greatly influenced by the burial. The notation TM and TE waves will be used to denote* the wave components with horizontal magnetic vector and horizontal electric vector respectively. Table 1 indicates some characteristics of the waves from buried dipoles and from a reference quarter wavelength monopole set on the earth. The latter is a useful basis for comparison. It has approximately -3 dB gain with respect to isotropic at 10° elevation angle.

---

*Another notation for TM and TE is vertically and horizontally polarized respectively.

Dipole antennas, including a small loop which is a magnetic dipole, are considered almost exclusively. The following notation will be used:

VED, vertical electric dipole;
VMD, vertical magnetic dipole;
HED, horizontal electric dipole;
HMD, horizontal magnetic dipole.

A buried vertical dipole gives a weaker field throughout the air space than does a buried horizontal dipole, other things being equal, and the dielectric constant, ε', of the ground being greater than 2, which is almost always the case. This is due to the cone of emission from the ground into the air space (fig. 1). For $\varepsilon' = 6$ the cone angular radius is 24°. The vertical dipoles give no emission straight up and at 24° the underground pattern factor of the dipole is 8 dB weaker than the maximum, which occurs in the broadside direction.

The buried horizontal dipole sends maximum energy straight up. The horizontally traveling surface wave is emitted at 24° from maximum of the dipole, for both the TE and TM polarizations, causing at most 0.7 dB loss due to the underground pattern factor of the dipole at 24° from broadside, ε being 6.

For any antenna system the field strength decreases at low elevation angles, as indicated in table 1. At low angles the buried antenna exhibits an approximately constant loss compared to an antenna on the surface, see last line of table 1. This extra loss due to burial is explained in sections C and D below. The loss is about 30 dB for TM wave and 40 dB for TE waves at 1° elevation angle, ε' being 6. The TM wave is almost always stronger than the TE wave and is therefore more useful. Also it gives a ground wave, useful for nearby on-the-ground reception.

Power gain is defined in the footnote of table 1.

Table 1. Fields of a monopole, and various dipoles buried in earth, with dielectric constant = 6 and conductivity = 0.003 S/m, stated relative to an isotropic emitter. Depth is assumed zero. The eighth line shows the depth attenuation per meter.

Antenna	TM/TE Character	Power Gain[a] 10° Elevation	1° Elevation	2° Elevation
λ/4 monopole with λ/2 radius metal ground plane	TM	∿ -3 dB	∿ -18 dB	∿ -14 dB
Buried VED	TM	-21.8 dB	-38.7 dB	-33.0 dB
Buried VMD	TE	-25.9 dB	-46.1 dB	-40.2 dB
Buried HED	TM	-14.6 dB	-31.7 dB	-26.1 dB
	TE	-19.0 dB	-38.3 dB	∿ -32.6 dB
Buried HMD	TM	-13.8 dB	-30.9 dB	-25.4 dB
	TE	-19.8 dB	-39.1 dB	-33.3 dB
1 meter depth absorption	TE,TM	-2.19 dB	-2.20 dB	- 2.20 dB
Buried HED relative to surface monopole	TM	-11.6 dB	-13.7 dB	-12.1 dB

(a) The power gain of an antenna at any angle is the ratio of the power density observed to the theoretical power density that would have been furnished by an isotropic emitter in free space at the same distance.

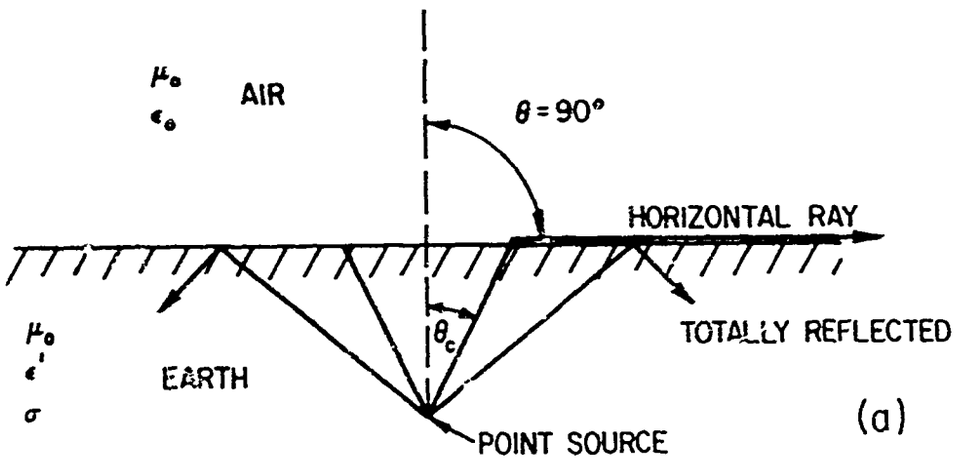

$\epsilon^* = \epsilon' + i\frac{\sigma}{\omega\epsilon_0} \equiv n^2$; $\theta_c = \arcsin(1/n)$

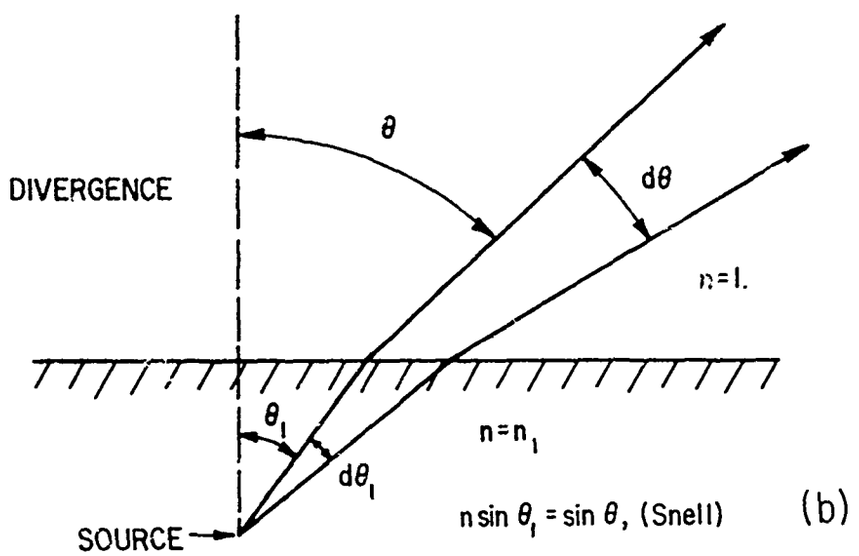

Figure 1, a. Rays at critical angle; b. divergence.*

*Long captions for all figures are given in the "List of Figures". The caption accompanying each figure will usually be abbreviated.

C. THEORETICAL DERIVATION OF THE PATTERN GAIN

A convenient summary of buried antenna theory is that of Hufford [1]. Earlier results include [2], [3], [4]. The Sommerfeld method for a dipole in a half space is used. The final results are given below. The notation is as follows:

ε_0, μ_0 are the constitutive parameters of free space.

In the ground $\mu_1 = \mu_0$, and the complex refractive index, n, is given by

$$n^2 = \varepsilon_1/\varepsilon_0 = \varepsilon' + i\,\sigma/(\omega\varepsilon_0);\ \text{also}\ \varepsilon^* = \varepsilon_1/\varepsilon_0.$$

$$\sigma = \text{conductivity, S/m.}$$

$$k_0 = \omega(\mu_0\varepsilon_0)^{\frac{1}{2}},\quad Z_0 = \sqrt{\mu_0/\varepsilon_0},$$

$$k_1 = nk_0,\quad Z_1 = Z_0/n,$$

$$\sin\theta_1 = \sin\theta/n\quad \text{(complex Snell's law)},$$

$$\cos\theta_1 = (n^2-\sin^2\theta)^{\frac{1}{2}}/n,$$

$$\text{loss tangent} = \varepsilon''/\varepsilon' = \sigma/(\varepsilon'\varepsilon_0\omega),\ \omega = 2\pi f.$$

A ray at the critical angle of incidence in the ground, θ_c, emerges horizontally with $\sin\theta = 1$ in the air, figure 1a, thus

$$\sin\theta_c = 1/n,\ \cos\theta_c = (n^2-1)^{\frac{1}{2}}/n.$$

The equations for the far fields in the air at a height greater than a few wavelengths, due to dipoles buried in a flat earth (half space), for TE and TM waves respectively, are stated relative to the field of an isotropic emitter in free space as follows [1]:

$$E_e/E_f = L\ C_e\ D\ A_e$$

$$E_m/E_f = L\ C_m\ D\ A_m$$

$$L = 2/(\mathrm{Re}\ n)^{\frac{1}{2}}$$

$$D = \exp\left(i\ k_o\ h(n\cos\theta_1-\cos\theta)\right)$$

$$C_e = \cos\theta/(n\cos\theta_1+\cos\theta)$$

$$C_m = \cos\theta/(\cos\theta_1+n\cos\theta), \qquad (1)$$

where

$$A_e = 0, \quad \text{VED}$$
$$A_m = -i(3/2)^{\frac{1}{2}} \sin \theta_1, \quad \text{VED} \tag{2}$$

$$A_e = i(3/2)^{\frac{1}{2}} \cos \phi, \quad \text{HED}$$
$$A_m = i(3/2)^{\frac{1}{2}} \cos \theta_1 \sin \phi, \quad \text{HED} \tag{3}$$

$$A_e = i\, n/|n| \times (3/2)^{\frac{1}{2}} \sin \theta_1, \quad \text{VMD}$$
$$A_m = 0, \quad \text{VMD} \tag{4}$$

$$A_e = -i\, n/|n| \times (3/2)^{\frac{1}{2}} \cos \theta_1 \sin \phi, \quad \text{HMD}$$
$$A_m = i\, n/|n| \times (3/2)^{\frac{1}{2}} \cos \phi, \quad \text{HMD} \tag{5}$$

ϕ = the azimuth angle measured from an axis that is perpendicular to the horizontal dipoles.

Equations (2) to (5) are equations (7.18), (7.19), (7.23), and (7.24) of [1]. The product LCD of equation (1) would be used for a buried isotropic point source. The factor A represents the effects of coupling the dipole pattern to the angular cone of emission. The field E_f of an isotropic emitter of power W watts in free space is

$$E_f = (W\, Z_0/4\pi R^2)^{\frac{1}{2}} \ \text{V/m, rms}$$
$$= (30\, W)^{\frac{1}{2}}/R. \tag{6}$$

The range R is measured in meters.

The simplicity and utility of Hufford's normalization (to an isotropic source) should be noted. Many of the theoretical formulations give the field pattern for a dipole with a specified current or a specified dipole moment, which leaves the reader with some work to do, to find the current or moment from the power. By the present method [1] from W and R, the E field of an isotropic source is found from equation (6), assuming 100 percent efficiency. Then one applies the gain pattern of the buried source, equations (1)-(5), and gets the predicted field in the air.

The predicted ground wave is found in the same way using equations (18)-(20), section E, below.

D. PHYSICAL OPTICS OF BURIED ANTENNAS, [9]

It is instructive to try to obtain the transmitted far field based on physical optics. There are three main steps: one step is to find the power transmission factor of the interface using plane wave concepts; a second step is to obtain the change in the spherical wave divergence factor at the interface, considering the point source aspects; and the third step is to calculate the absorption in the ground.

The interface transmission coefficient may be found from Fresnel's equations and conservation of energy. The refractive index is temporarily assumed to be real, and losses are added later. The power transmission coefficients for a plane wave in the dense medium refracted into the vacuum (air) are:

$$T_e^2 = \frac{4n \cos \theta_1 \cos \theta}{(n \cos \theta_1 + \cos \theta)^2}, \tag{7}$$

$$T_m^2 = \frac{4n \cos \theta_1 \cos \theta}{(\cos \theta_1 + n \cos \theta)^2}, \tag{8}$$

where e and m denote TE and TM waves respectively. These are obtained from Fresnel's field equation, section 9.5 of [5], taking into account changes of the impedance and the area of a beam at an interface.

Considering the spherical wave from an elementary doublet as a bundle of rays we find the change in the solid angle due to refraction into the air space, figure 1. The spherical angles are

$$d\Omega_1 = \sin \theta_1 d\theta_1 d\phi_1, \text{ in the earth}$$
$$d\Omega = \sin \theta d\theta d\phi, \text{ in the air.} \tag{9}$$

It is true that

$$d\phi_1 = d\phi. \tag{10}$$

From Snell's law

$$\sin\theta = n \sin\theta_1, \tag{11}$$

and by differentials

$$\cos\theta d\theta = n \cos\theta_1 d\theta_1. \tag{12}$$

Using equation (10) and equation (12) in equation (9) we have

$$d\Omega = \sin\theta d\phi_1 \; n \cos\theta_1 d\theta_1/\cos\theta. \tag{13}$$

The power per solid angle in the air relative to the power per solid angle in medium 1 is the power gain of the interface transmitting into the air. Denoting this as $p_{12,e}$ for a TE mode wave

$$p_{12,e} = \frac{p_0 \; 4n \cos\theta_1 \cos\theta}{(n\cos\theta_1+\cos\theta)^2 \sin\theta d\phi_1 \; n\cos\theta_1 d\theta_1/\cos\theta} \div \frac{p_0}{\sin\theta_1 d\theta_1 d\phi_1}$$

$$p_{12,e} = \frac{4\cos^2\theta}{(n\cos\theta_1+\cos\theta)^2 \; n} \tag{14}$$

Likewise for the TM case

$$p_{12,m} = \frac{4\cos^2\theta}{(\cos\theta_1+n\cos\theta)^2 \; n} \tag{15}$$

Equations (14) and (15) are identical to $(L\,C_e)^2$ and $(L\,C_m)^2$ of equations (1) using a real refractive index. The inclusion of complex n and θ_1 requires that the squares be replaced by absolute values squared.

The pattern factor A of a dipole in the ground includes $\sqrt{3/2}$, and $\sin\theta_1$ for vertical dipoles, $\cos\theta_1$ for horizontal dipoles, end fire, and a sine or cosine of ϕ appears, see equations (2) to (5).

Finally the attenuation in the ground may be obtained approximately from the propagation factor in the ground and the ray optical distance,

$$D' = e^{ik_1 d/\cos\theta_1'}, \tag{16}$$

where $k_1 = k_0 n$ is the complex wave number and θ_1' is a real angle defined as the direction of a plane wave refracted by the ground using the velocity in the ground, c/n'. An approximate Snell's law with this assumption is

$$\sin\theta_1' = n'^{-1}\sin\theta, \tag{17}$$

where n' is the real part of the complex refractive index of the ground. The attenuations given by D of equations (1) and by D' of equation (16) are nearly the same in spite of the different forms. The attenuation exponent in equation (16) becomes 1 percent greater than in equations (1) when the loss* tangent is 0.6. A correct electromagnetic treatment of equation (16) is given in section 9.8 of reference [5] as well as in [1].

E. GROUND WAVE

The ground wave ($\theta = 90°$) is obtained from a Sommerfeld type of theory. Equations (1) are replaced by [1],

$$\begin{aligned} E_e/E_f &= S_e U_e\, DA_e/(-ik_0 R) \\ E_m/E_f &= S_m U_m\, DA_m/(-ik_0 R), \end{aligned} \tag{18}$$

where R is the horizontal distance to the field point, and

$$\begin{aligned} S_e &= 2/\left((\mathrm{Re}\ n)^{\frac{1}{2}} \times (n^2-1)\right), \\ S_m &= 2\, n^3/\left((\mathrm{Re}\ n)^{\frac{1}{2}} \times (n^2-1)\right), \end{aligned} \tag{19}$$

*Provided also $\varepsilon' > 5$.

$$U_e = 1 - i\, k_0\, z\, Z_0 \cos\theta_c / Z_1,$$
$$U_m = 1 - i\, k_0\, z\, Z_1 \cos\theta_c / Z_0, \qquad (20)$$

where z is the height of the field point above the interface; z is restricted to a few wavelengths. At greater heights the space wave approximation, equations (1), are used. Equations (18) state that the ground wave field decays at 1/R relative to the reference field E_f which already decays as 1/R, equation (6). The ground wave is not important when the receiving station is an aircraft. There is evidence of the ground wave in the field trials described below. The receiving tower was 30.5 m horizontally from the point of burial. The theoretical loss at low angles is greater than that observed at low angles. For example, the gain at 2° elevation angle should be approximately 12 dB less than the gain at 10° elevation angle. The experiments show approximately a 6 dB difference. We therefore usually discuss results at 10° elevation angle. Another evidence of the ground wave occurs in figure 11. With no ground wave the results for the two reference monopoles would nearly coincide, as in figure 9. The ground wave, stronger at lower frequencies, shows clearly as a difference in the fields at low angles.

F. CALCULATION OF THE FIELD FROM EQUATIONS (1)

A computer program was written to evaluate the field in the air of a buried dipole, from equations (1). The important factor from these equations for low-angle reception is LC which, as we have seen in section 2D, arises from divergence and from the Fresnel transmission. The power gain due to LC combined with the broadside power gain of a dipole, 1.5, will be denoted as the interface gain, I. However, the term interface loss will also be used for I. Figure 2 shows the TM wave interface loss in dB, at certain angles, versus ε' of the earth. Specifically the curves give the value in dB of

$$I = 1.5|LC|^2 = 6 \cos^2\theta / (n'|\cos\theta_1 + n \cos\theta|^2).$$

The transformation from the buried dipole to the air space is often adequately represented by f, since depth attenuation and underground pattern factor may be taken as zero dB.

The next factor considered is depth attenuation computed from $|D|^2$ in equations (1). Figure 3 shows the depth attenuation in dB/m for a range of ground conditions.

There are some simple factors remaining to obtain a complete evaluation of equations (1):

1. The azimuthal variation of a horizontal dipole is either $\sin \phi$ or $\cos \phi$ as indicated in equations (2)-(5).
2. The vertical dipole has an important factor $|\sin \theta_1|^2$, see figure 4. (This factor is sufficient to remove the fully buried vertical dipole from consideration for high ε'; however, partial burial will be discussed.)
3. The horizontal dipole has a factor $|\cos^2 \theta_1|$ for the end fire component. This is of interest for the TM wave from the HED. It is a small factor under usual conditions (fig. 4).

In summary, figures 2, 3, 4 can be used to determine the loss (neglecting inefficiency) of the TM wave from a buried horizontal elementary dipole, or a buried VED.

The graphs, which concentrate on low elevation angles, are based entirely on equations (1). For the TE wave emitted end fire from a HMD use figures 3, 4, and 5. The TE and TM waves emitted broadside from the horizontal electric and magnetic dipoles do not suffer the underground pattern factor, figure 4.

An example of using the curves may be useful. Consider the TM wave of a horizontal electric dipole buried 0.1 m deep in ground with $\varepsilon' = 10$ and $\sigma = 0.01$ S/m. The receiving point is at 2° elevation angle. We sum the following losses

Interface loss (fig. 2)	27.0 dB
Depth attenuation (fig. 3)	0.55 dB
Underground pattern (fig. 4)	0.45 dB
Total loss	28.0 dB

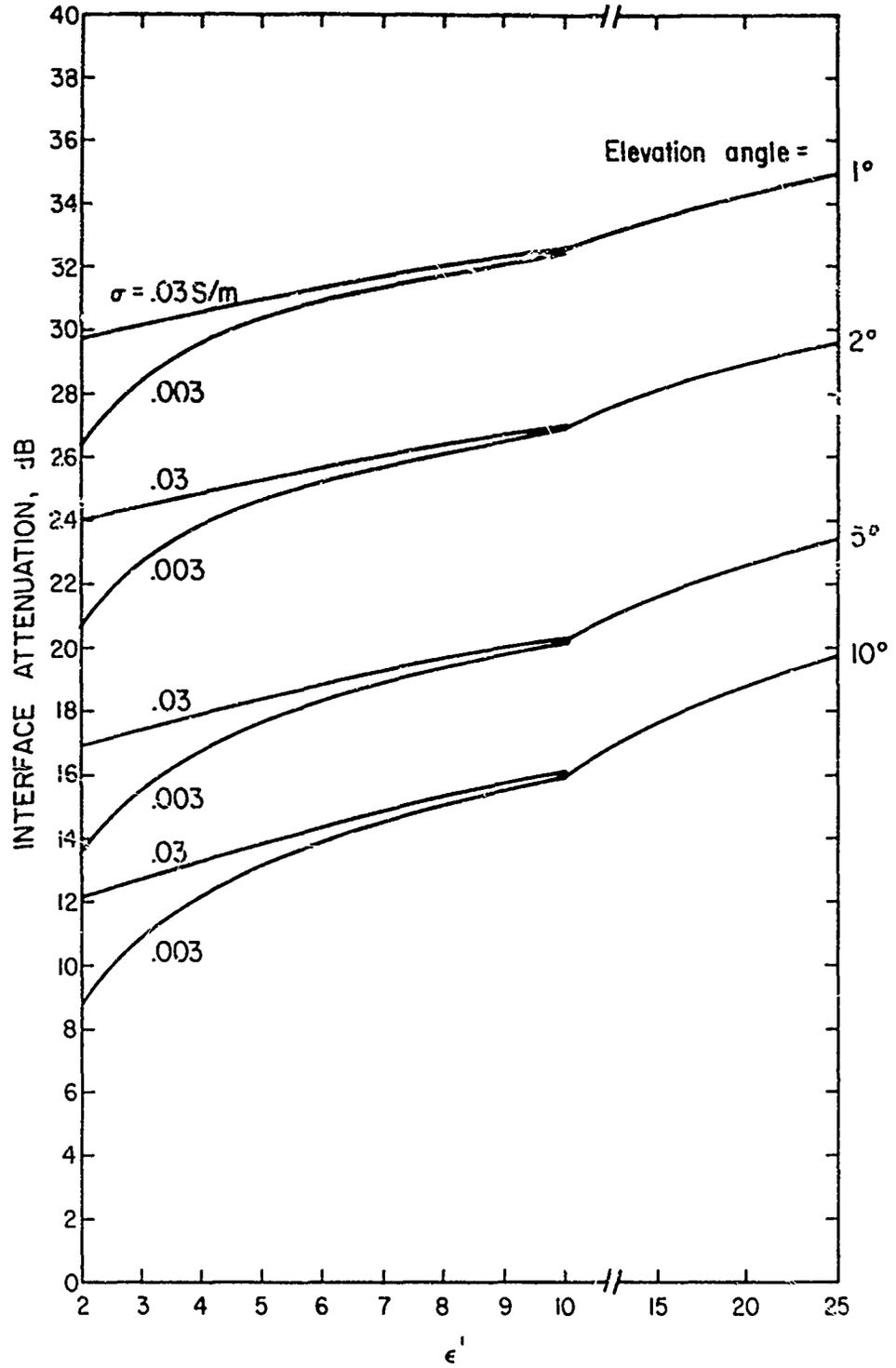

Figure 2. Interface-divergence loss of TM wave.

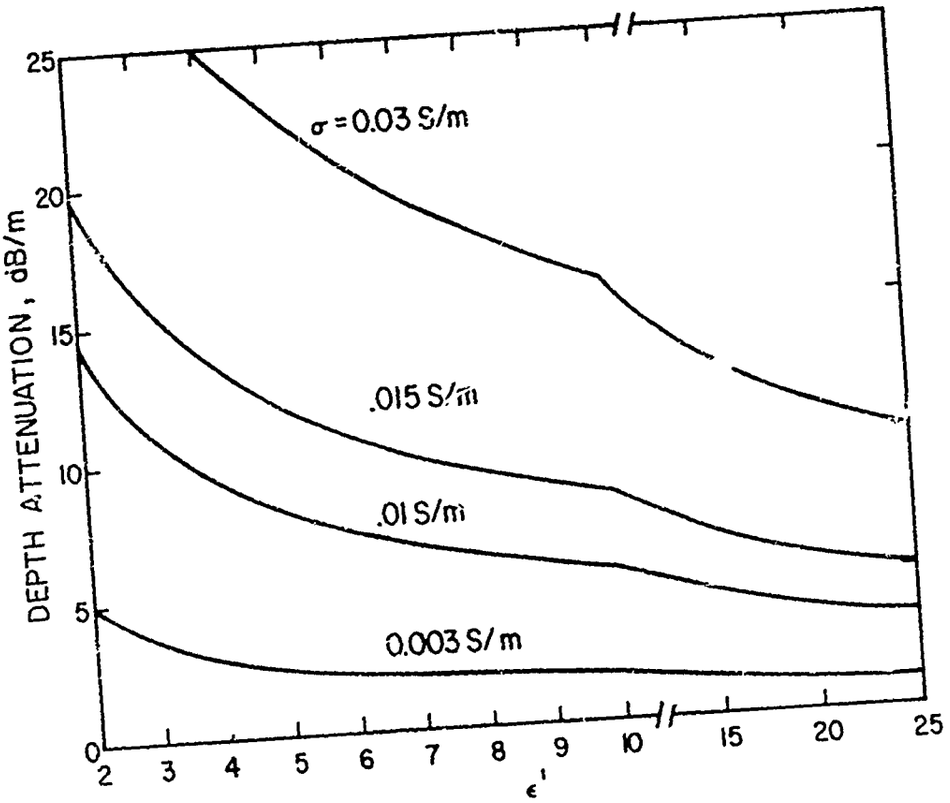

Figure 3. Depth Attenuation.

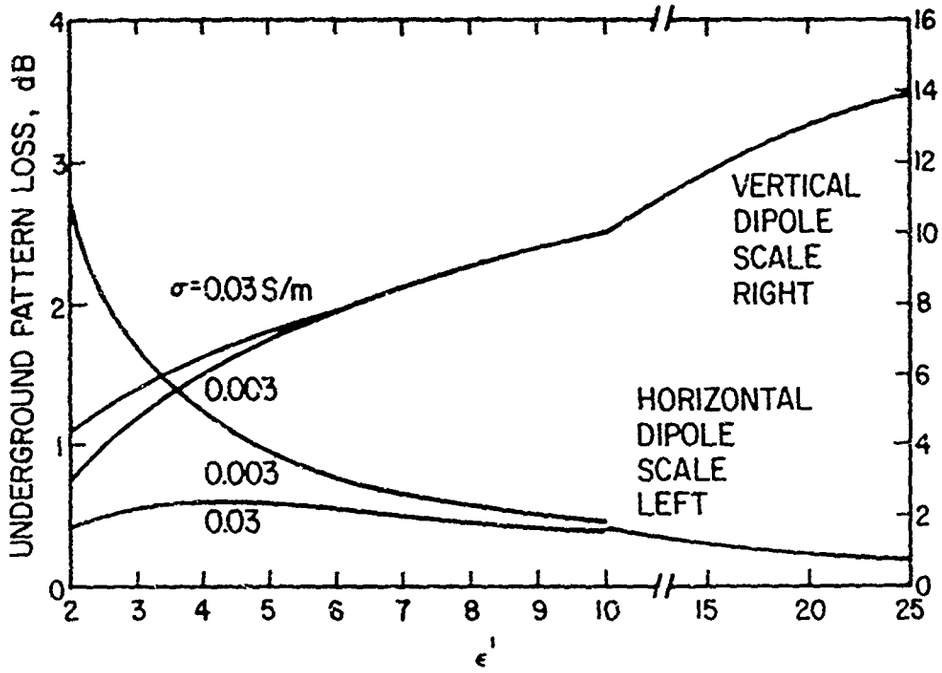

Figure 4. Underground pattern loss.

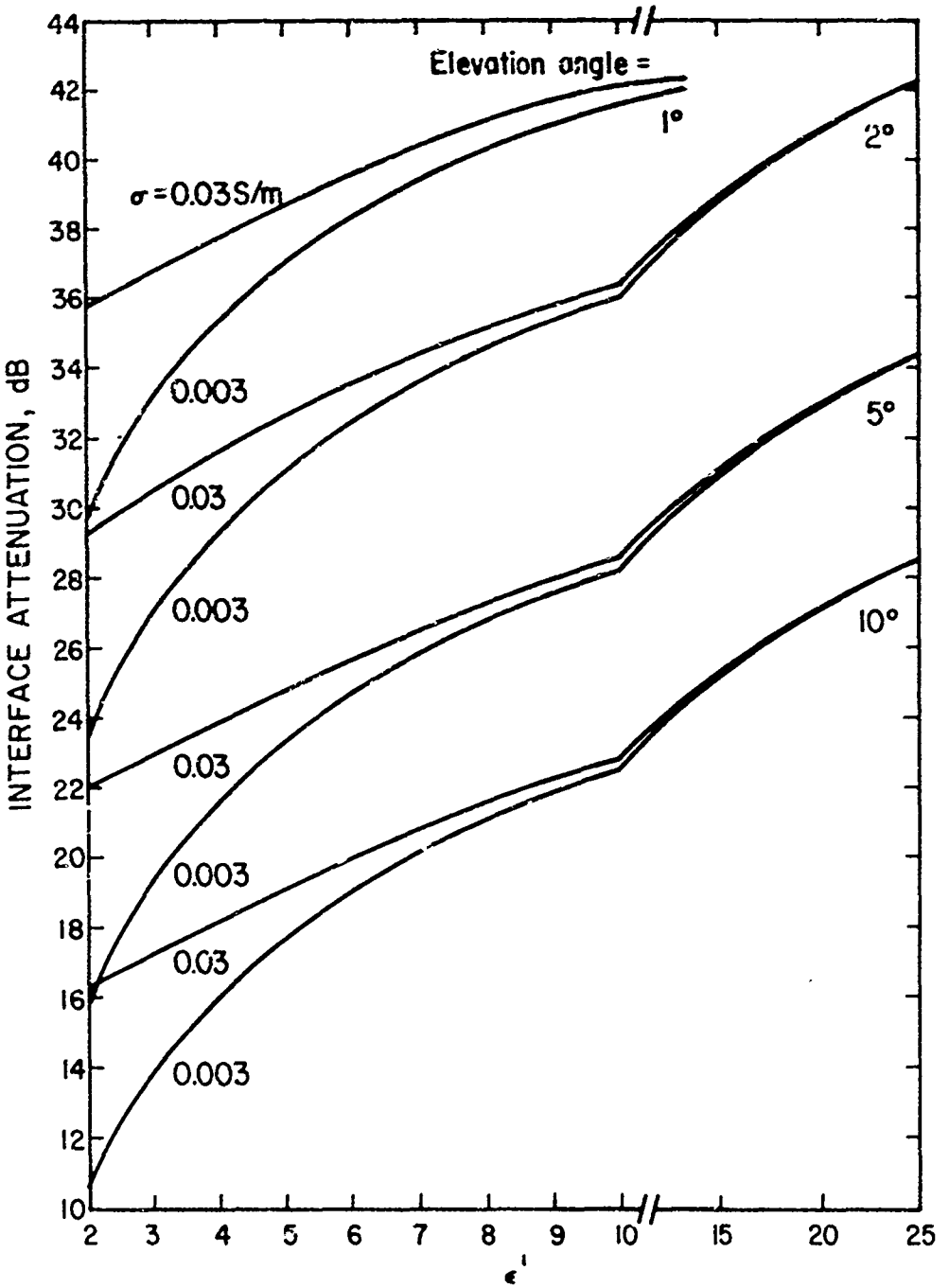

Figure 5. Interface-divergence loss of TE wave.

At an elevation angle of 10°.

Interface loss (fig. 2)----------	16.0 dB
Depth Attenuation (computer)-------	0.54 dB
Underground pattern (computer)-----	0.44 dB
Total loss	16.98 dB

The main factor during shallow burial will be the interface loss, and it depends strongly on the elevation angle.

The TM wave from a horizontal magnetic dipole (HMD) has a small advantage over that from the HED in that the underground pattern factor is zero dB.

Figure 4 shows that the vertical dipoles have more loss than the horizontal dipoles. This is because the vertical dipole is working mainly end fire in exciting the interface within the critical angle θ_c.

G. EFFICIENCY

The received field strength also depends on the efficiency of the antenna, which is influenced by burial. Efficiency will be treated experimentally, below.

3. EXPERIMENTS COMPARED TO EQUATIONS (1)

A. INTRODUCTION

Experiments were carried out initially mainly to verify the theory contained in equations (1). Later, the main purpose was to develop resonant antennas where the focus is on efficiency, impedance, Q factor, and ground effects on these. The comparison with theory was quite satisfactory, thus allowing the main emphasis to be on the resonant antenna development in the later work which is described in sections 4 and 5.

The agreement of the experiments with the theory contained in equations (1) occurs mainly in two areas:

(1) The predicted absolute value of the fields relative to an isotropic source are approximately correct, including the fact that the TE waves are weaker than TM waves.

(2) The gain pattern as a function of elevation angle is approximately correct.

The remainder of this section describes the experimental measurement method and illustrates results that yield the above conclusions.

Figure 6 shows the main elements of an experimental system for measuring [8] field strength and antenna gain.

B. TRANSMITTED POWER

Direction couplers measure the forward and reverse power, denoted as P_1 and P_2 respectively. The attenuation (fig. 7) of the RG-9 cable of length u was measured at 72° and 32°F using a network analyzer. The curve shown for 50°F was interpolated.

Assuming that the directivity of the two couplers is infinite, the power delivered to the antenna is

$$P_a = P_1 \, 10^{-dB_c/10} - P_2 \, 10^{+dB_c/10}, \qquad (21)$$

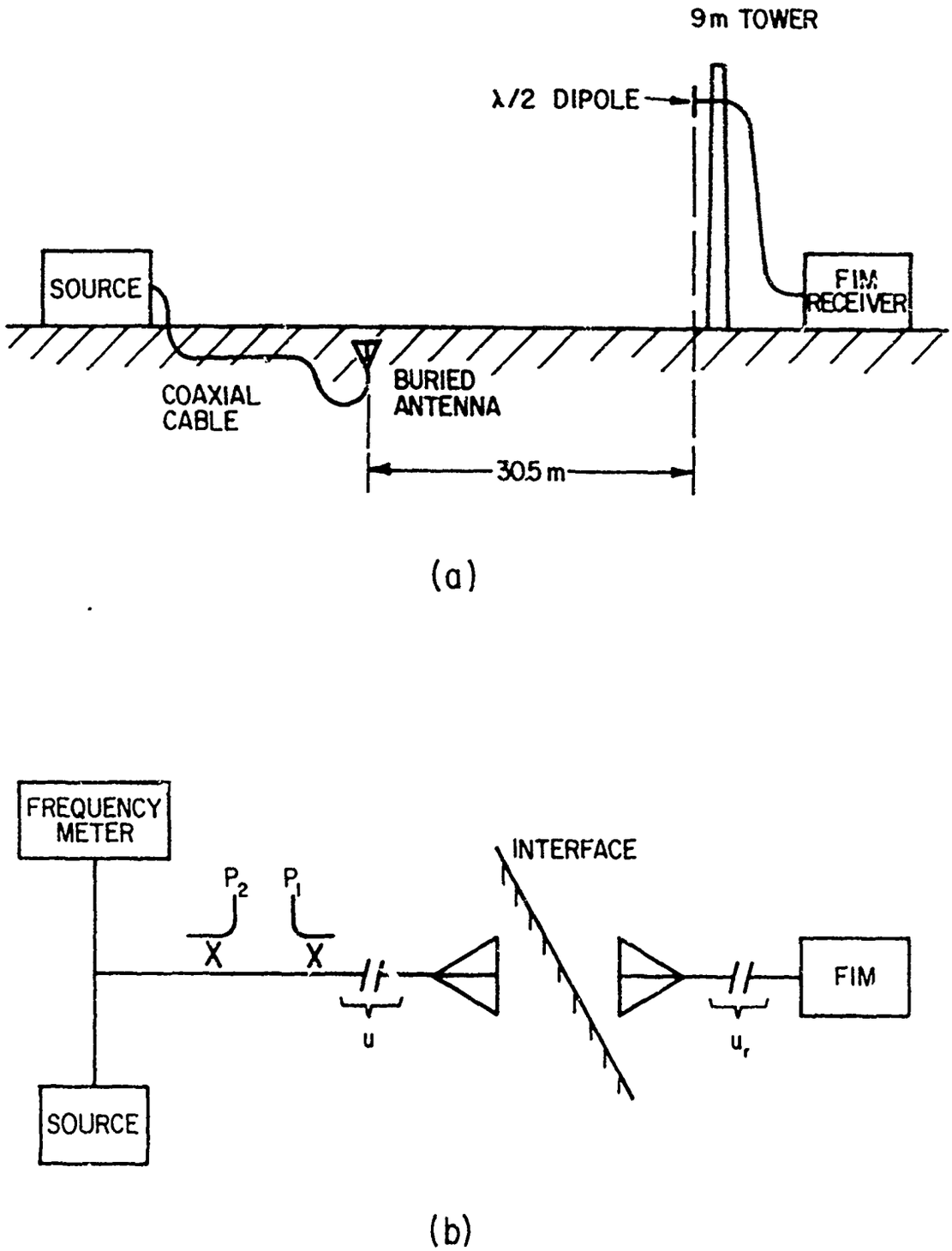

Figure 6. Experimental system for field measurements.

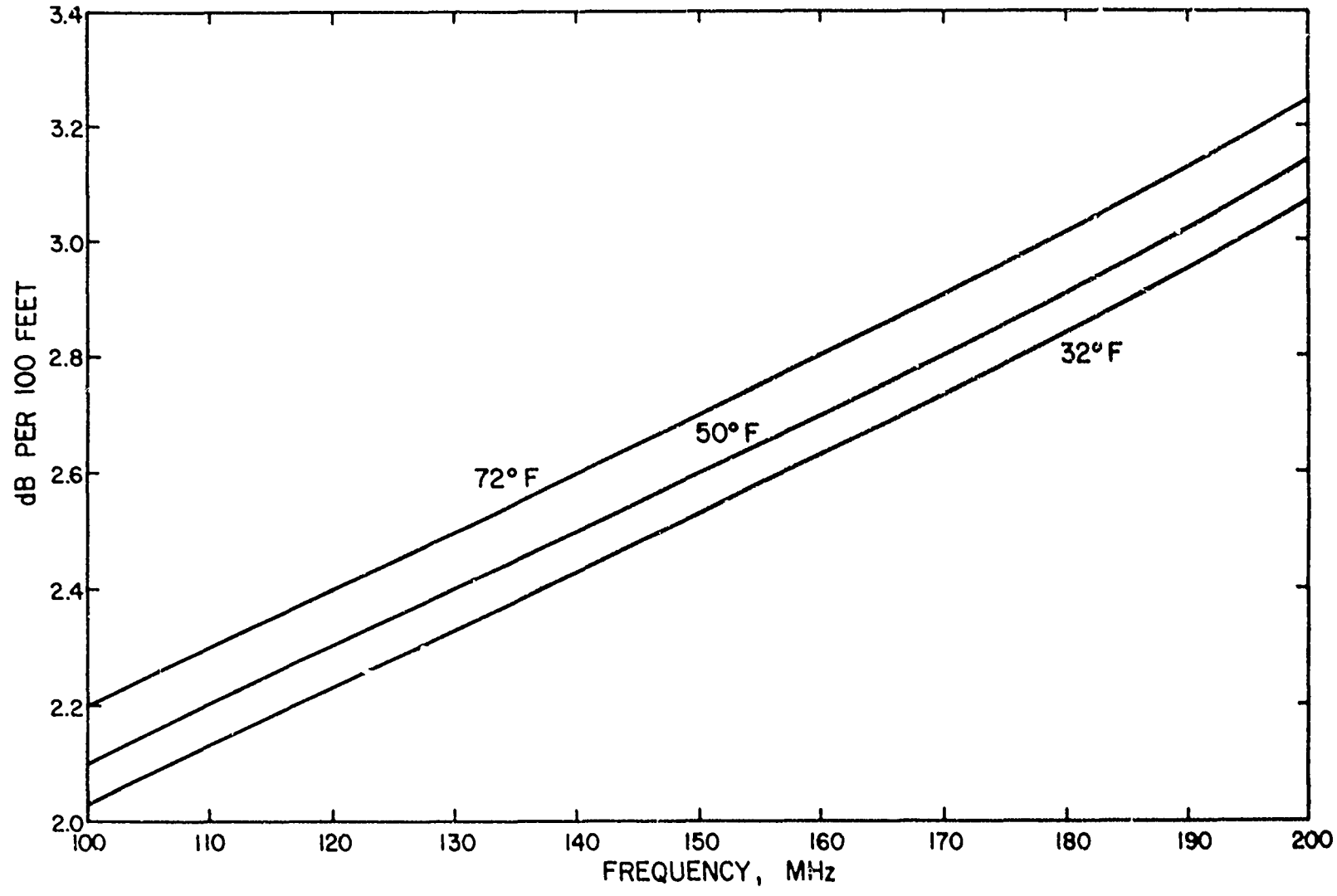

Figure 7. Measured one-way attenuation of cable.

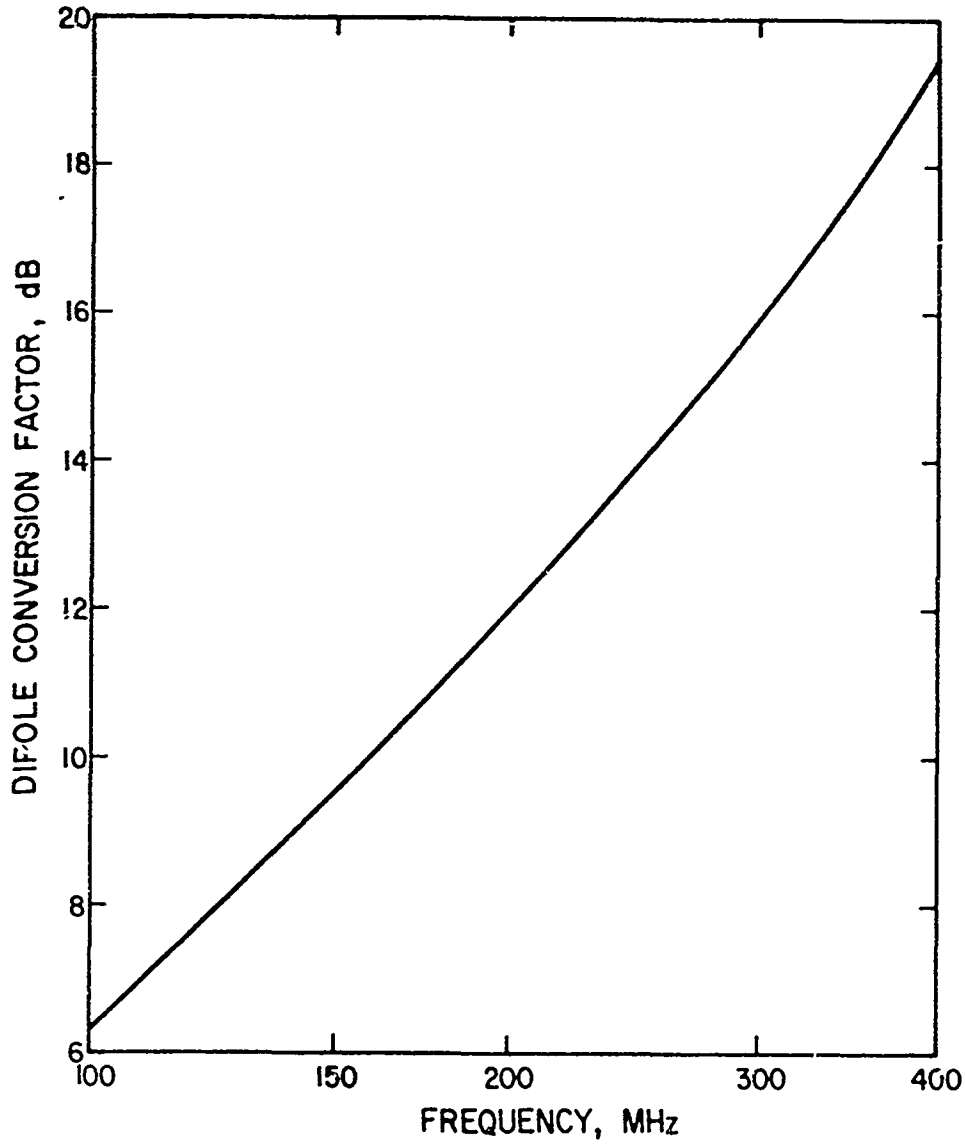

Figure 8. Field strength conversion factor of receiver.

where dB_c is the one way attenuation of the cable with reflectionless terminations.

The radiated power, P_r, is P_a multiplied by the efficiency, J, of the antenna

$$P_r = J\ P_a. \tag{22}$$

The efficiency of an antenna is the ratio of radiated power to the total input power, which consists of ohmic heating power plus radiated power

$$J = P_r/P_t = P_r/(P_r+P_{cu}), \tag{23}$$

where P_{cu} denotes ohmic heating power.

The efficiency of the antennas was measured and estimated, as will be discussed in section 4E.

C. FIELD STRENGTH CALIBRATION

The field intensity meter (FIM) at the receiving terminal consists of a calibrated rf voltmeter and its associated antenna and cable of known characteristics and calibration factors. The rf voltmeter had an internal calibration system. This was recalibrated and corrected where necessary.* The antenna and impedance factors were measured by the NBS standard field method [6], with results as shown in figure 8. At 145 MHz the factor is 9.3 dB, which can be approximately explained as follows:

1. The effective length conversion factor, from the field in V/m to the voltage across an open circuited half wave dipole is λ/π, or -3.63 dB at 145 MHz.
2. The conversion from an open circuited generator to a matched load, the receiver, is 0.5 in voltage or -6 dB.
3. A conversion factor, arising from the mismatch of the antenna and receiver to the cable, and consequent interactions, is unknown.

*This calibration includes the loss of the cable.

The sum of factors 1 and 2 nearly equals the measured conversion factor, -9.3 dB, which implies that the third factor was small.

D. COMPARISON OF THEORY AND EXPERIMENT FOR A "REFERENCE" MONOPOLE

A quantitative comparison using the rather predictable field of a "reference" monopole adds considerable confidence to the evaluation of unknown HF and VHF antennas. (The term reference is in quotes. The gain pattern of this type of antenna has shown good agreement between theory and experiment.) The so-called reference monopole is a quarter wavelength slim wire antenna on a ground plane one wavelength in diameter set on the earth. Available well-developed theory [7] is then applied to predict the space wave over an earth with dielectric parameters ε' and σ. The use of a reference monopole in compact range experiments, as in the present work, thus provides a check on the transmitted power calibration and the FIM calibration described above. Figure 9 exhibits the theoretical far-field power gain pattern of the reference monopoles at two frequencies, for certain ground constants.

Measurements to be compared with theory were made at a rented alfalfa field site, 5 miles east of Boulder, Colorado. The horizontal distance from the monopole antenna to the receiver tower (fig. 6) was 100 feet (30.5 m).

Table 2 gives the steps in comparing the theoretically calculated field and the measured field of reference monopole antennas at 145 and 300 MHz. The comparison is made at an elevation angle of 10° where the field is less dependent on surface imperfections and surface waves than at low angles.

The predicted and measured voltmeter readings with all conversion factors taken into account are seen to agree to within 1 dB.

Table 2. Theoretical and measured field strengths of the reference monopole antennas at 145 and 300 MHz. The ground was dry, $\varepsilon' = 5.0 \pm 1.0$ at the surface. Elevation angle of receiving point is 10°.

Frequency	145 MHz	300 MHz
Theoretical field[a] at 30.5 m of 1 W isotropic source, dB > 1 μV/m	105.1	105.1
Resonant dipole field strength conversion factor (fig. 8)	-9.3 dB	-16.0 dB
Theoretical[b] gain pattern factor at 10°, $\varepsilon' = 5$, $\sigma = 0.05$ S/m	-3.1 dB	-3.0 dB
Predicted voltage of receiver, dB > 1 uV (theoretical).	92.7 dB	86.1 dB
Measured voltage at 10° elevation	101.5 dB	90.7 dB
Conversion to 1 W source[c]	-11.0 dB	-7.0 dB
Transmitter cable and VSWR factor,	+1.5 dB	+2.1 dB
Experimental 10° reading converted to 1 W radiated	92.0 dB	85.8 dB

(a) From equation (6).

(b) Reference [7].

(c) At 145 MHz P_1 is 12.56 W; 5 W were indicated but the directional coupler was -4 dB from the rated value at 145 Mc. At 300 Mc P_1 is 5 W. Values of P_2 are 0.32 W and 0.19 W at 145 and 300 MHz respectively.

From this close agreement we conclude that the transmitted power, the FIM voltage, and the cable attenuations have been accurately determined. It is estimated that the power delivered to the antenna and the field strength at the receiving antenna are being measured with an accuracy of ± 1.0 dB.

E. FAR FIELD PATTERN VERSUS ELEVATION ANGLE

The height dependence of the field pattern is quite similar for a buried source and for the monopole set on the interface. As shown in table 3, the theoretical patterns differ by nearly a constant ratio (constant number of dB), and the difference is due to interface loss plus depth attenuation. We may say that the buried antenna becomes, to a good approximation, a weakened virtual monopole on the surface.

The presentation in table 3 makes it clear that loss due to burial at low angles is mainly an interface loss, plus depth attenuation if present, and not a change in shape of the space wave pattern compared to the pattern of a monopole at the interface.

F. MEASURED LOSS OF RATHER IDEAL BURIED DIPOLES

Experiments were done to check the loss of a buried horizontal dipole against the theory [1].

A sleeved dipole was constructed using handbook values of length and diameter to attain resonance at 145 MHz and an impedance of 50 ohms. The dipole diameter was 2.5 cm and the length was 98 cm. The dipole was contained in a 10 cm diameter lucite tube to reduce the effect on the resonant frequency of the surrounding ground.

The dipole was buried as a HED 15 cm below the surface. The TM wave was received in the end fire direction.

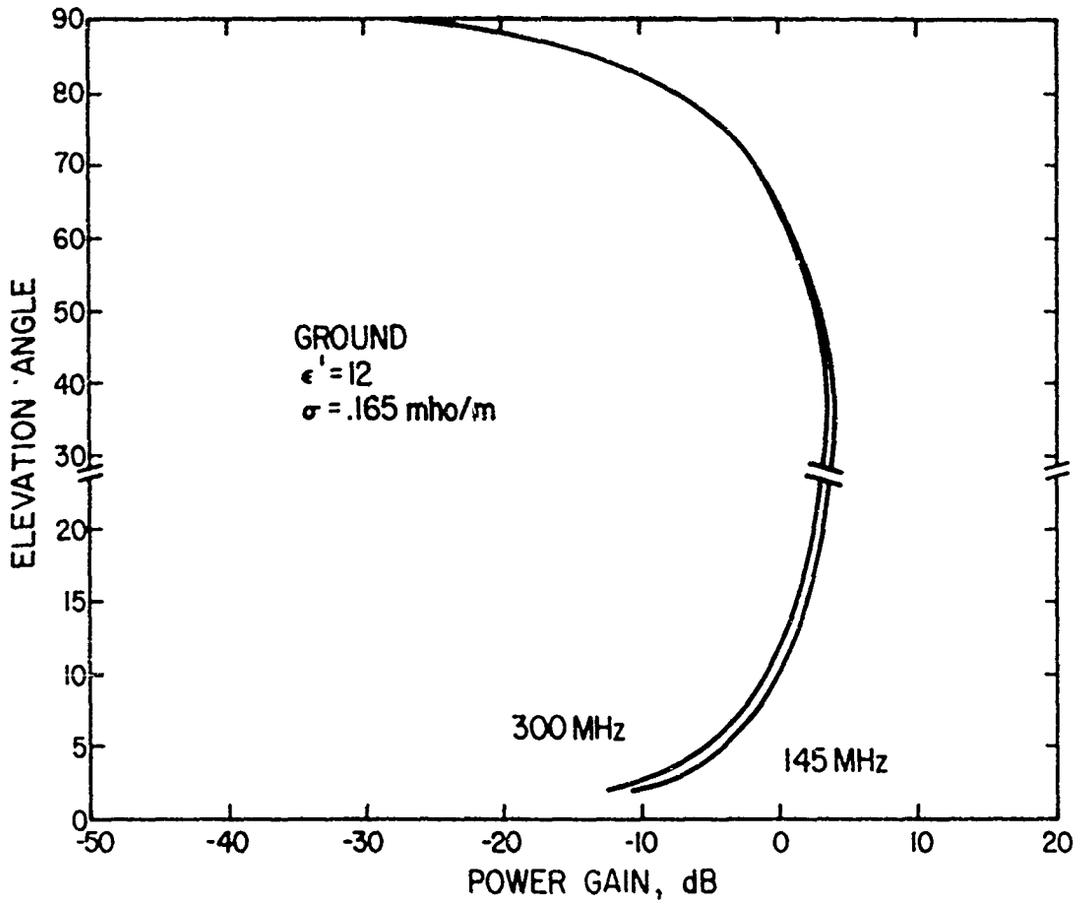

Figure 9. Theoretical far-field pattern of monopole.

Table 3. TM-wave gain pattern of a "reference" monopole set on the interface and of a buried horizontal magnetic dipole (interface gain only, depth loss is zero). Ground constants are $\varepsilon' = 10$, $\sigma = 0.03$ S/m; frequency = 145 MHz.

Elevation Angle	dB Gain, Reference Monopole[a]	Interface dB Gain of HMD[b]	dB Difference
2	-12.28	-27.01	14.73
4	-7.16	-21.86	14.70
6	-4.46	-19.14	14.68
8	-2.75	-17.38	14.63
10	-1.53	-16.13	14.60

(a) Reference [7], by an approximate calculation.

(b) Only the interface gain is given. Depth attenuation would be nearly constant versus angle, see figure 3.

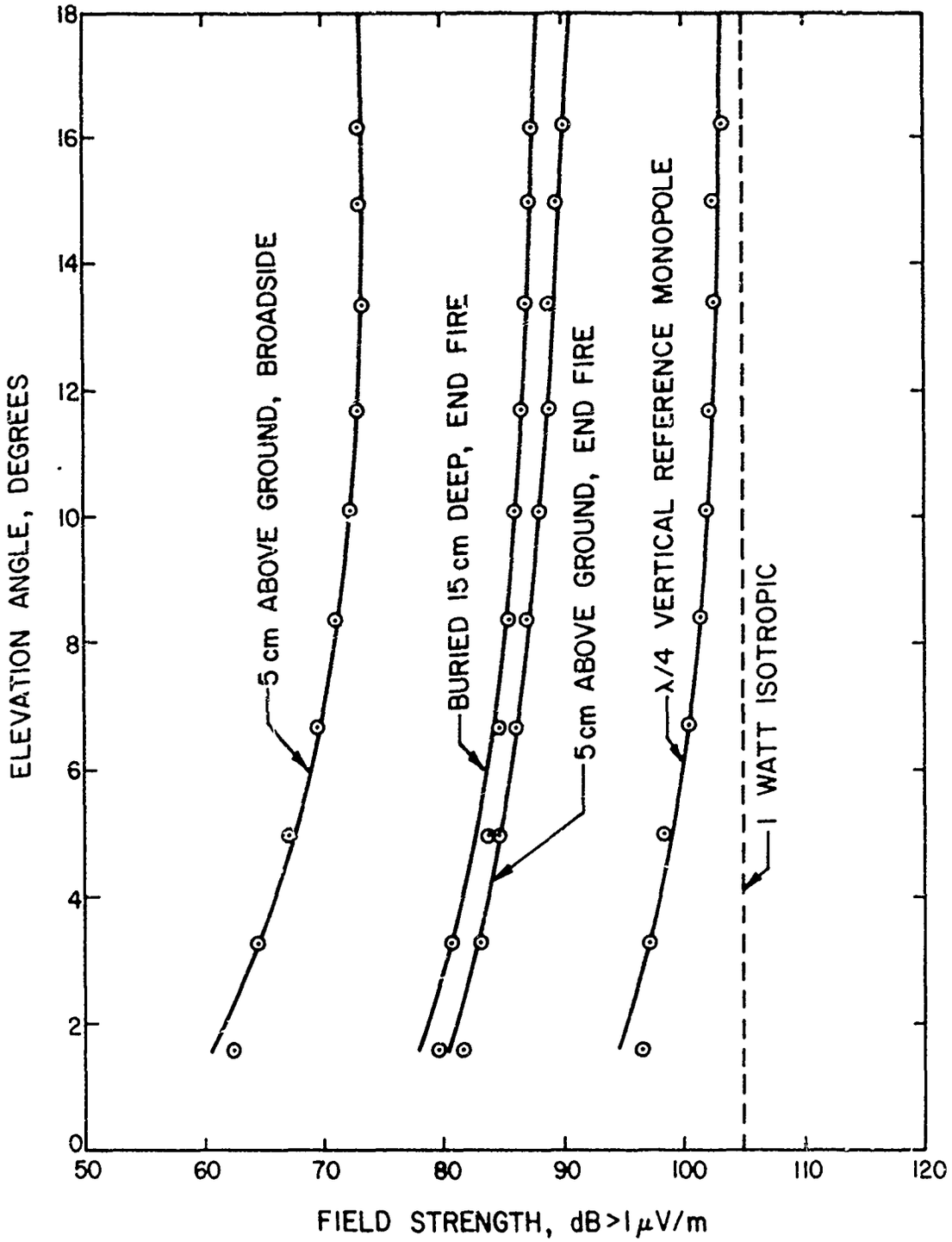

Figure 10. Measured field of monopole and buried dipole.

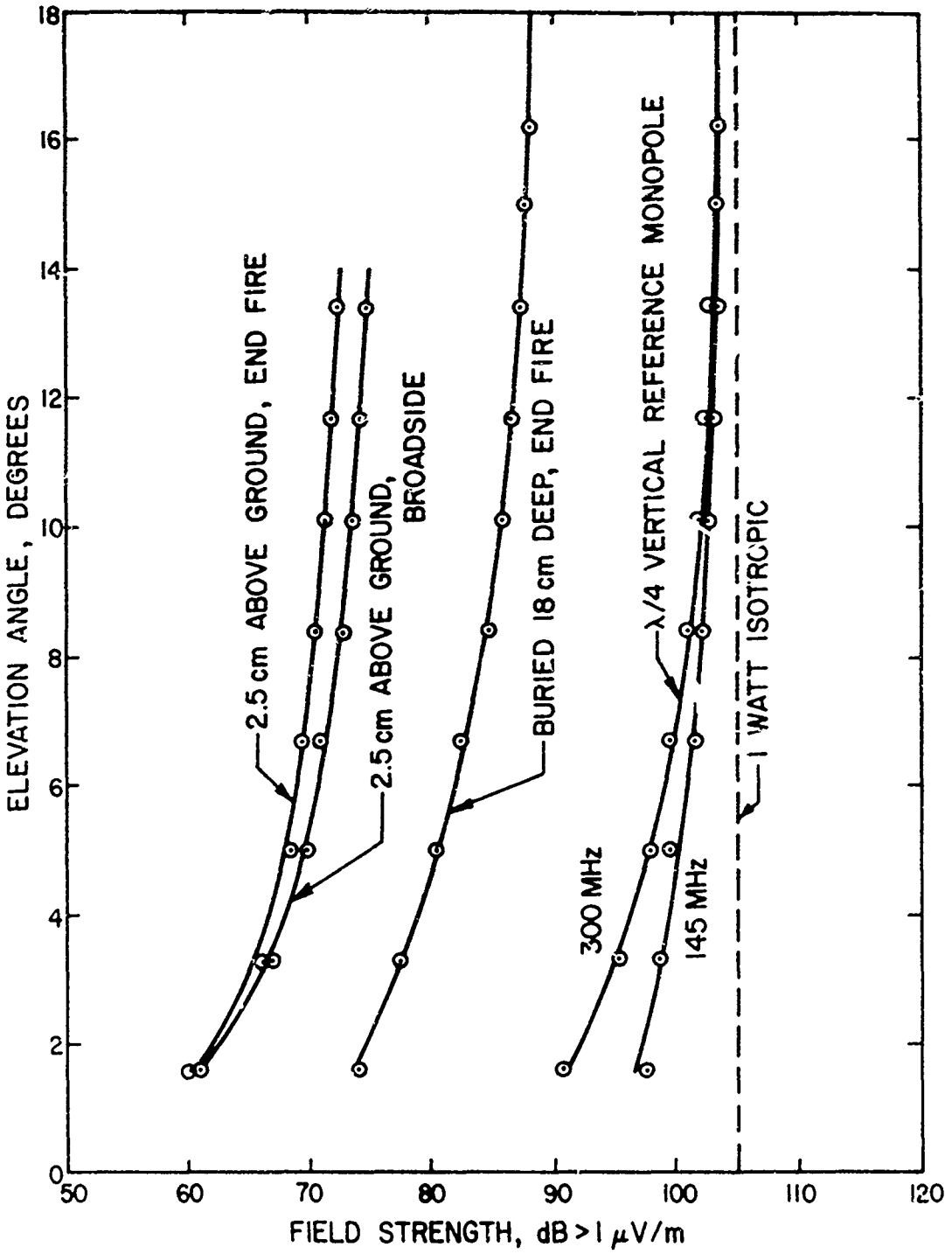

Figure 11. Measured field of monopole and buried dipole.

The dielectric constant of the undisturbed ground (quite wet), based on a core sample, was approximately 13. The disturbed dielectric constant of the dug-up ground is estimated as 10.

The estimated theoretical end-fire loss of a buried horizontal electric dipole, $\varepsilon' = 10$, $\sigma = 0.068$ S/m, at 10° elevation, relative to an isotropic emitter, from figures 2, 3, and 4 is----------19 dB.

The measured loss in the same condition was--------19 dB.

Figure 10 shows curves for the sleeved dipole. The field strength of the end fire above-ground test is questionable.

Figure 11 gives results for a folded dipole at 300 MHz. The above-ground end fire results are quite weak, and thus do not agree with the sleeved dipole end fire above ground. For this buried dipole the loss at 10° elevation angle relative to an isotropic radiator is again 19 dB. The agreement with theory is very good, but does depend heavily on having assumed that ε' of the repacked dirt is 10.

G. EFFECT OF SHALLOW BURIAL

This section is concerned with the interface loss and the underground pattern loss, see figures 2, 4, and 5, as functions of the burial depth. (For simplicity, the depth loss is assumed to be negligible.) When an elementary dipole is raised above the interface, the field strength at low angles in the far field increases. The Sommerfeld height-gain function for this effect is [1]

$$E(z) \sim 1 - i\, k_0\, \delta\, z, \quad z \geq 0 \tag{24}$$

where z is the height, $\delta = Z_1 \cos \theta_c / Z_0$ for TM waves, and other symbols are defined above equations (1).

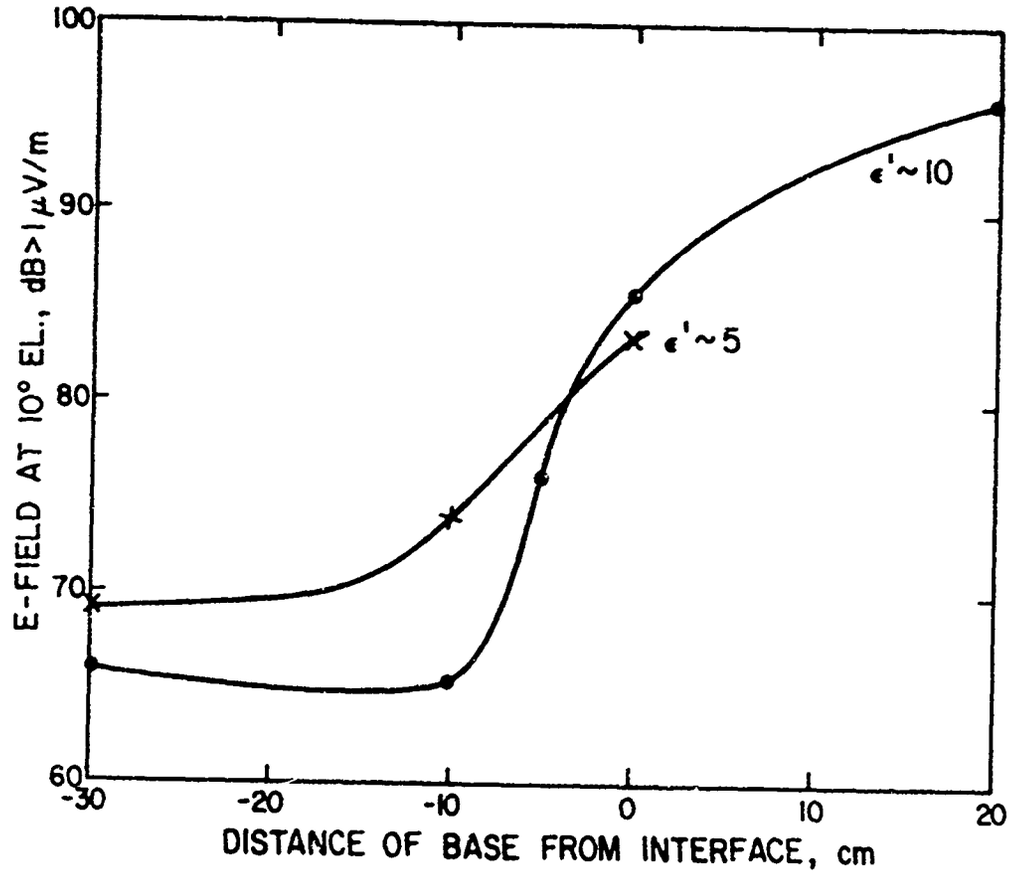

Figure 12. Field versus height of a VED.

When an encapsulated miniature dipole penetrates the earth the interface loss is initially less than would occur for a bare dipole because the encapsulant initially prevents the antenna from being covered. Figure 12 shows measured height (and depth) gain results for the A3 antenna (furnished by Frank Reggia, Harry Diamond Laboratories), a 2.54 cm length vertical monopole* on a 10 cm diameter ground plane. A polyfoam encapsulant 10 cm in diameter extends 2.54 cm above the top of the antenna.

The experimental curve shows that such a vertical monopole loses approximately 10 dB when the base is 5 cm below the interface, and approximately 20 dB when the base is well below the interface.

Equation (23) is not quantitatively obeyed above the interface in figure 12, probably due to the RG-9 cable feeding the bottom of the antenna. As the antenna is raised its effective length may increase due to the exposed cable.

The results in figure 12 suggest that a good candidate antenna is the low profile miniature vertical monopole on a small base plate, set in the ground with its top near the interface. The diameter of the base plate and encapsulant must be 4 or 5 times the height of the antenna, so that fairly low angle radiation can be emitted without intercepting the earth.

H. SUMMARY

Experiments using the "reference" monopole, see table 2, indicate that the experimental field measurements are quite accurate. Therefore, confidence can be placed in the characteristics of the buried antennas measured with the same system.

The experiments with rather ideal buried dipoles, as discussed in section F, indicate reasonable agreement with the theory of such buried antennas.

---

*The design is rather similar to that of antenna A8, figure 13. This type of antenna, a so-called monopole, is of course mainly a dipole because the ground plane is small compared to a wavelength.

It is therefore assumed that both the theory and the experimental measurements of the characteristics of buried antennas are well in hand. The remaining effort concentrates on practical construction and testing of miniature resonant antenna for burial.

Theory and experiment agree that buried dipoles exhibit considerable loss, except when ε' is small, as in dry sand. The low silhouette vertical monopole at the surface as described in section G has advantages of being simple and less lossy than fully buried designs. The monopole is further examined below.

4. DEVELOPMENT OF MINIATURE RESONANT ANTENNAS

A. INTRODUCTION

This section describes useful miniature antennas for burial, including principles of design and practical construction. The assigned frequency is 145 MHz and the allowed dimensions are a circular cylindrical form approximately 5 inches (12.7 cm) in diameter and of the order of 1 foot (30 cm) in length.

As concluded from the theory and theoretical comparisons, an ideally buried antenna has an unavoidable interface loss, I, as well as the smaller depth loss, and in some cases a small underground pattern loss (figs. 2, 3, 4, 5). The possibility of employing directive gain to counteract these losses was of course considered. Rather thorough reports on aperture antennas and traveling wave antennas with gain when buried [8], and arrays with gain [9], are available, but such methods are not suitable for the present purpose because of size and complicated burial requirements. Therefore the remaining task is to develop convenient miniaturized antennas for burial. The main concerns in designing the miniature antennas are as follows:

1. Impedance matching, coupling to the generator.
2. Efficiency.
3. Bandwidth.
4. Changes in the above as the capacitive stray field of the resonant antenna interacts with the burial medium.
5. Practicality and convenience.

B. CONSTRUCTION DETAILS

Figure 13 to 19 are schematic mechanical layouts for seven of the candidate antennas. In each case the antenna is built above an inverted copper cup, 12.7 cm in diameter and 12.7 cm

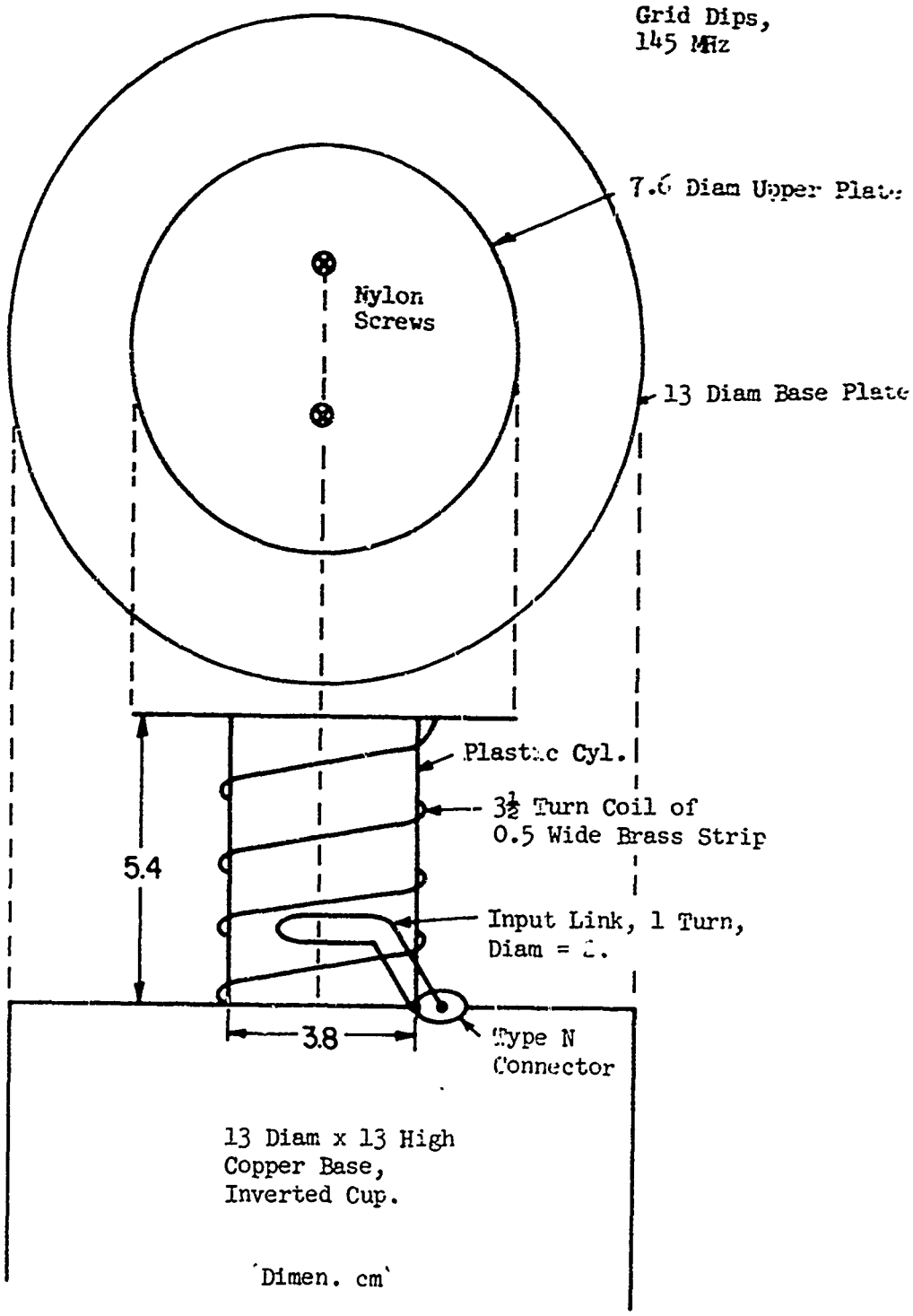

Figure 13. Vertical electric dipole, VED, A8.

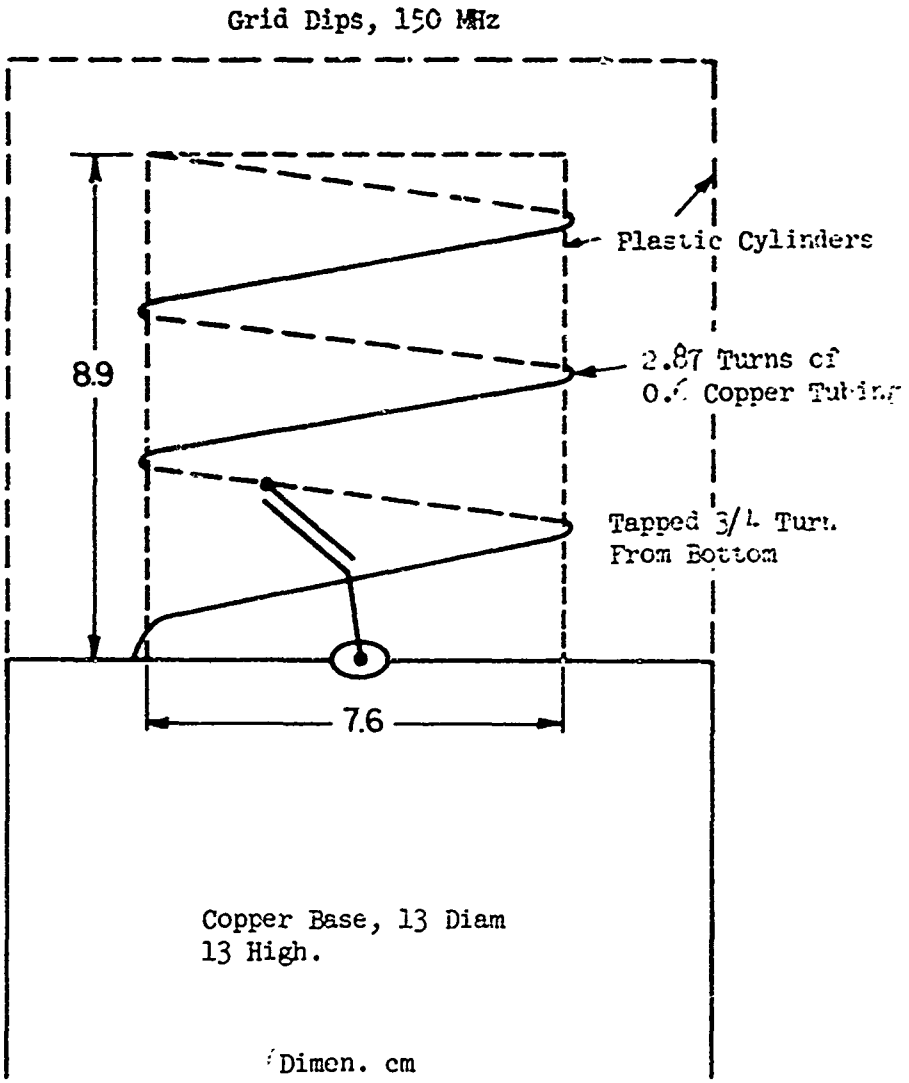

Figure 14. Antenna C4, a VED.

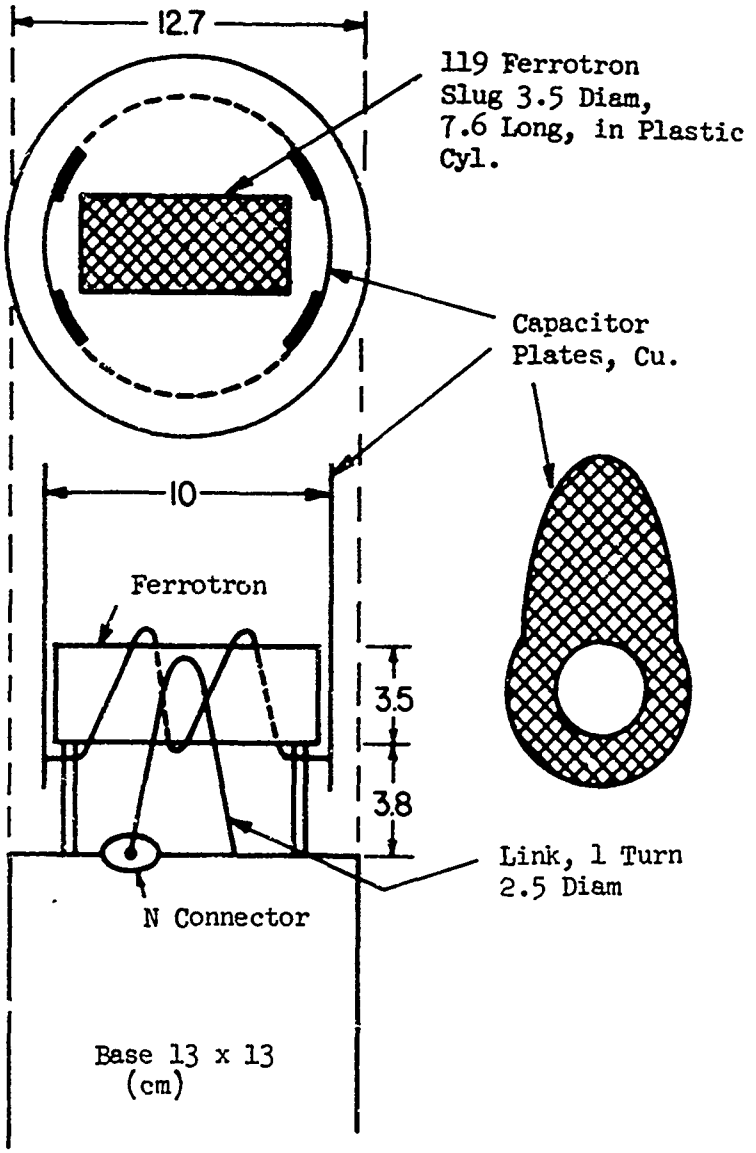

Figure 15. B3, a HED.

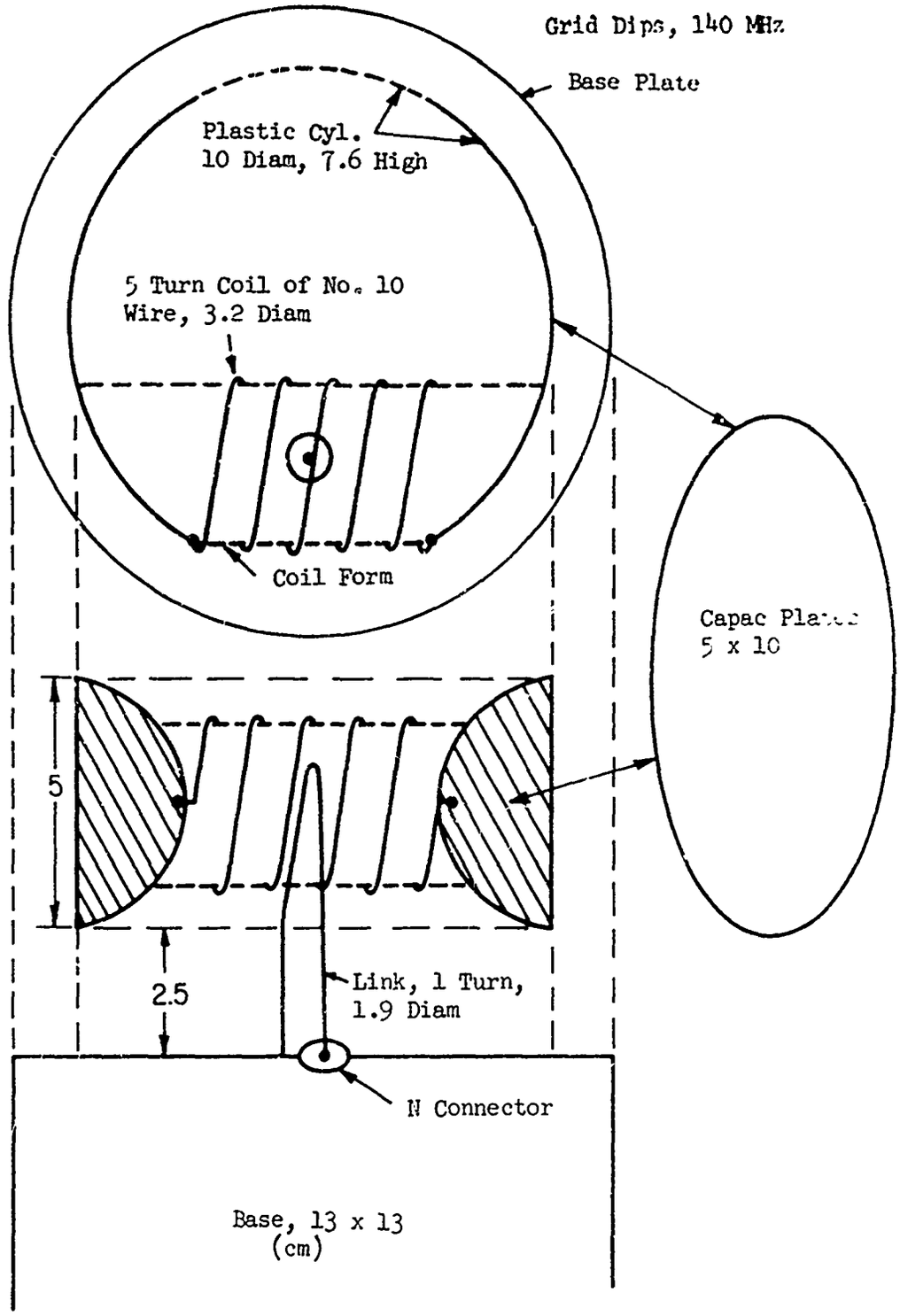

Figure 16. B4, a HED.

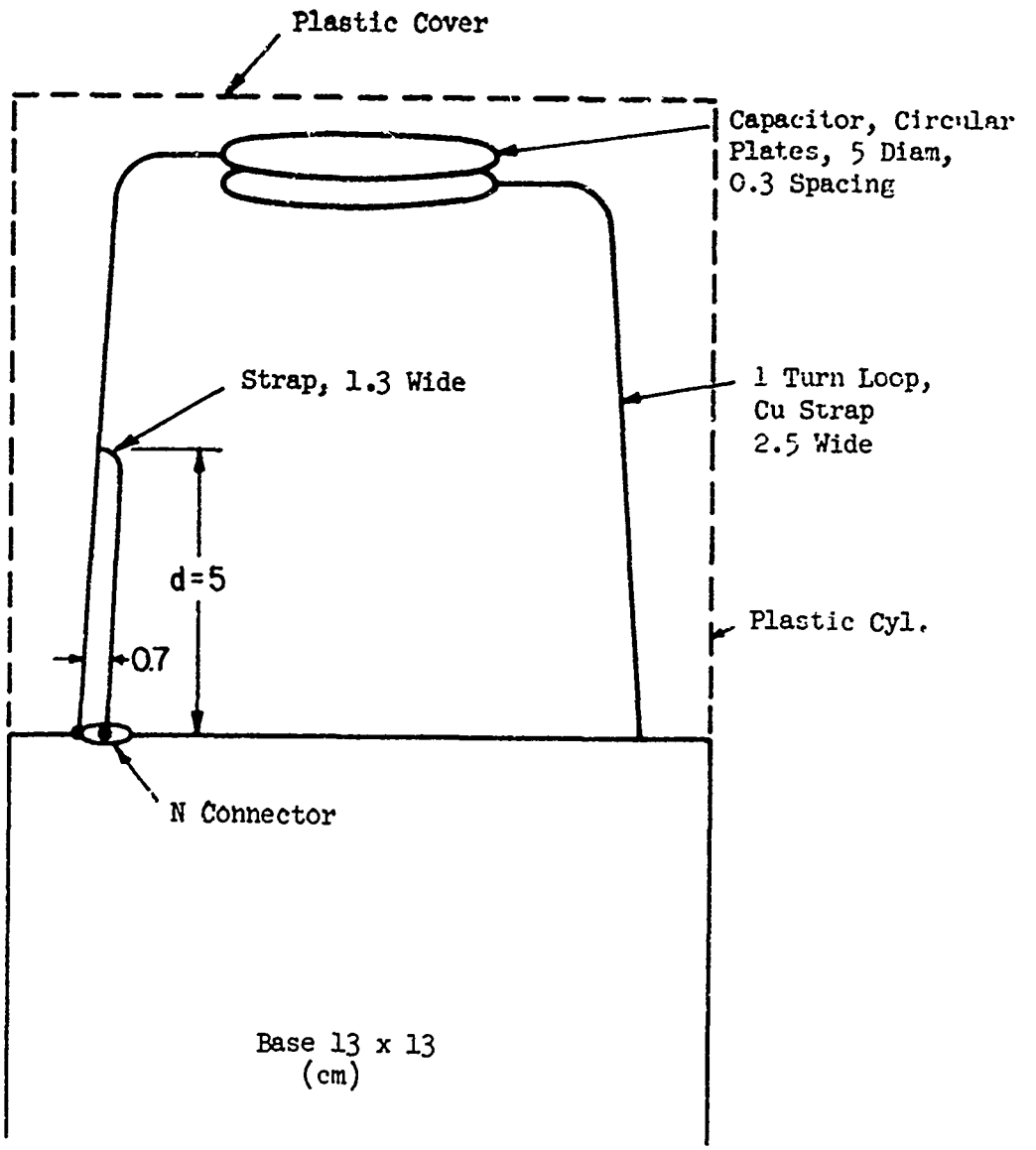

Figure 17. D3, a HMD.

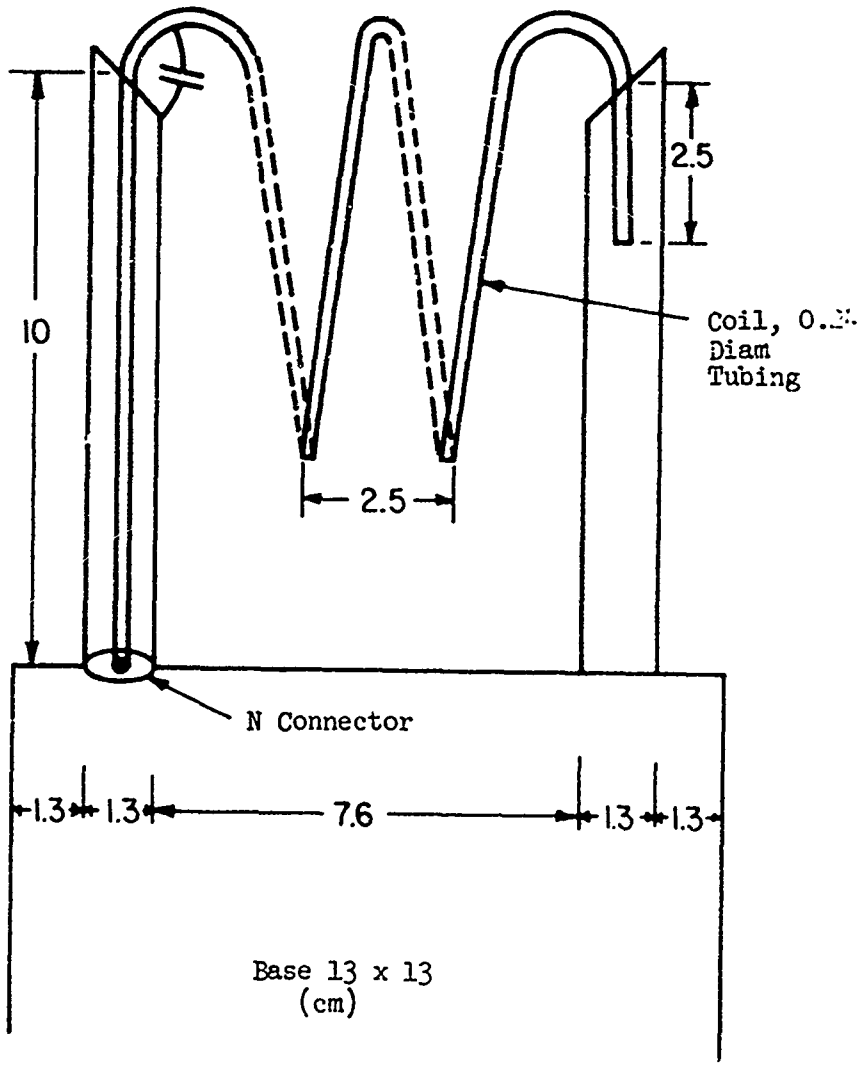

Figure 18. D4 (Pi-match antenna), HED-HMD.

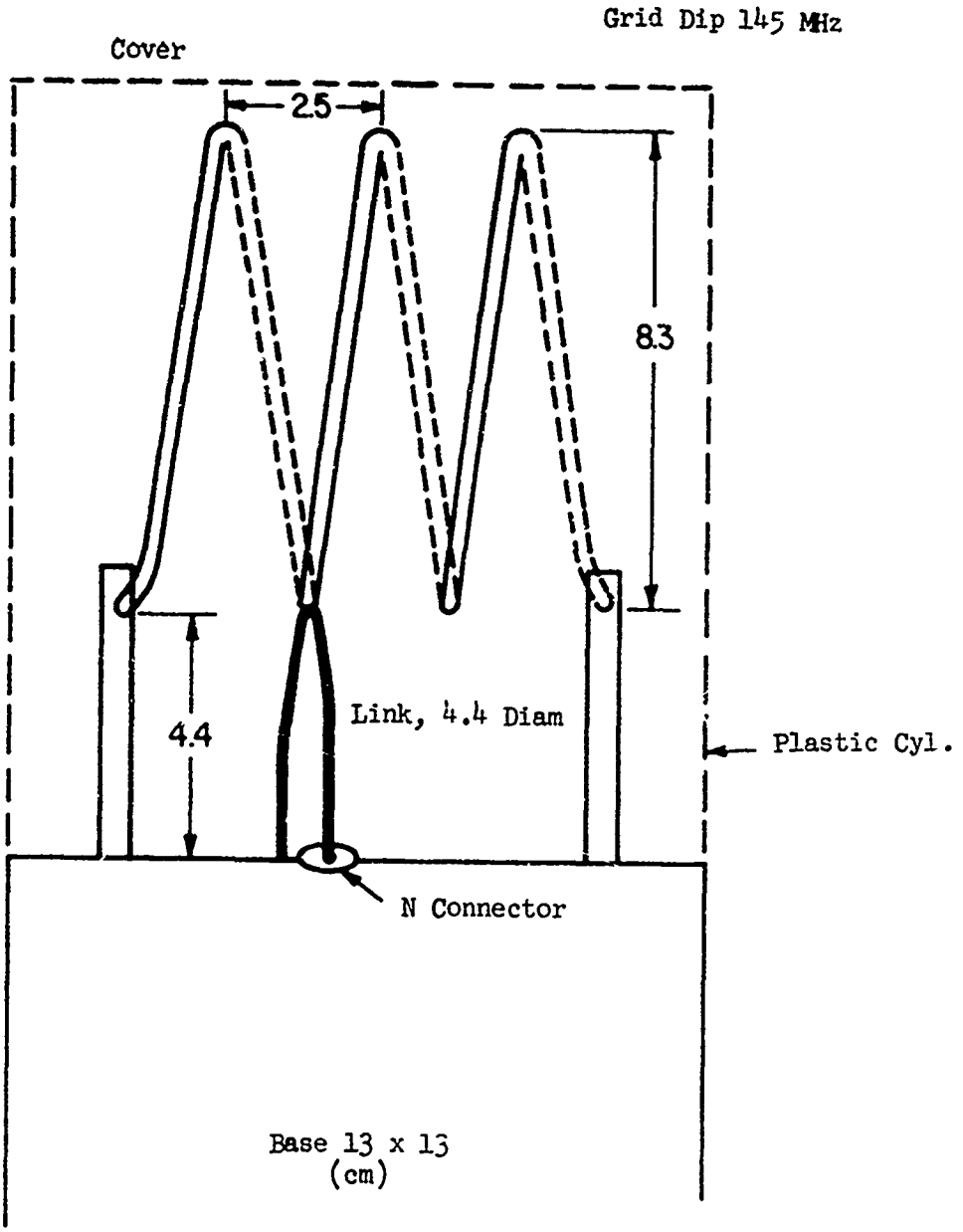

Figure 19. D5, HED and HMD.

in length (5" x 5") as a base. In each case the coupling consists of either a link which couples to the magnetic field of the antenna coil, or a tap on the coil. In each case a type N connector is mounted in the base near the feed point of the antenna. In our experiments the feed cable comes to the connector from below. In each case the antenna is "encapsulated" by setting a 12.7 cm diameter plastic cylinder over it with a top cover approximately 3 cm above the top of the antenna.

One requirement in design is to obtain a resonant frequency, near 145 MHz. This was obtained empirically. The size of the coil and the size of the capacitor plates at the ends of the coil were thus determined experimentally. Measurements of resonant frequency were made initially with a grid dip meter, and finally with the network analyzer; the latter tests will be described later.

Another requirement is to adjust the coupling coefficient of the antenna system for approximately 100% absorption of the energy from the transmission line. This adjustment requires that the antenna be critically coupled (which will be explained), which requires that the impedance be equal to that of the transmission line. The automatic network analyzer was the main instrument for studying the coupling.

C. IMPEDANCE MEASUREMENTS WITH THE NETWORK ANALYZER

Measurements of impedance versus frequency in the neighborhood of resonance may be analyzed to obtain the coupling coefficient, resonant frequency, and Q of a resonator. The antenna is a 1-port resonator insofar as the impedance measuring system is concerned. (Strictly it is a multiport resonator because it is coupled by radiation to the surrounding space.)

Impedances were measured with the antenna radiating into a small anechoic chamber near the automatic network analyzer. Calibration of the analyzer was obtained in the usual way by an

open circuit, short circuit, and pad successively connected to the end of the cable in the anechoic room. Then the antenna was connected to the cable and the complex impedance R + jX was measured at the plane of the connector. These results were plotted on the impedance circle charts for analysis. Figure 23 shows an example of the plots. The bandwidth, reflection coefficient and coupling coefficient, and frequency of resonance may be analyzed from the impedance plot. The main requirements are that the impedance curve pass near R = 50 ohm at the desired frequency and that the bandwidth be sufficient. The bandwidth is defined as the frequency separation of two points on the impedance curve at which the VSWR is 6:1, i.e. at which half of the power is reflected from the antenna (and half is accepted). Having exhibited the results qualitatively, we now go to a circuit analysis and a more quantitative analysis of the impedance data.

D. CIRCUIT REPRESENTATION AND Q ANALYSIS

Circuit analysis is useful in finding the antenna efficiency. Figure 20 shows two possible circuit representations of a resonator (the antenna) terminating a transmission line [10]. Part a. represents a series resonant circuit and part b. transforms to the parallel resonator circuit shown in c. The experimental data agreed with the parallel resonance, parts b. and c.

The measured impedance at the input to the primary inductor L_1 in figure 20b is given by the formula

$$Z = j\omega L_1 + (\omega M)^2/\left(R(1+j2Q_0\delta)\right) \tag{25}$$

where $\delta = (\omega-\omega_0)/\omega$, and the Q of the resonance is

$$Q_0 = R/\omega L. \tag{26}$$

The (angular) frequency of resonance is $\omega_0 = 2\pi f_0$, and ω is the test frequency. The first term in equation (25) is a shift

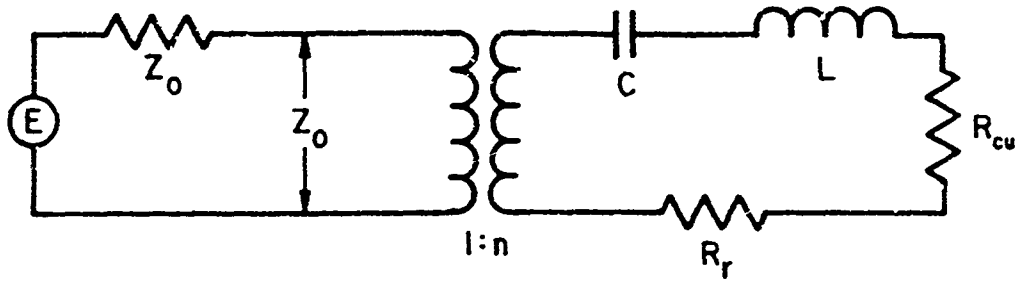

(a)

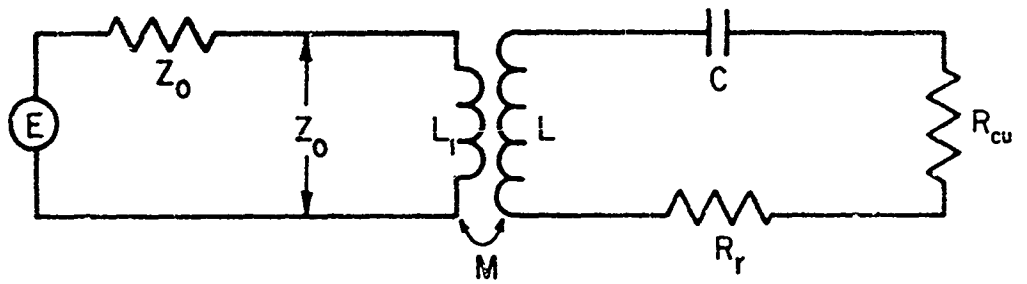

(b)

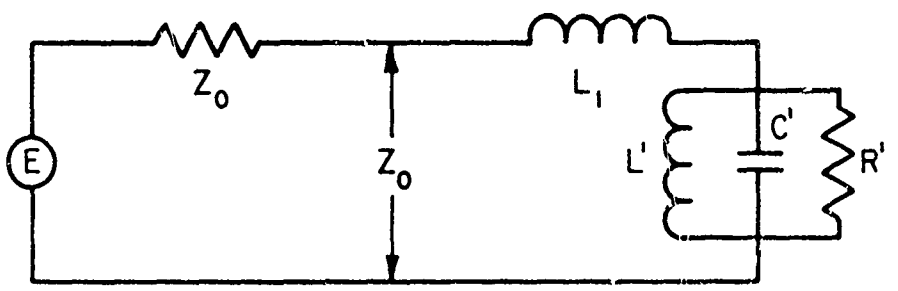

(c)

Figure 20. Circuit representations of a resonator coupled to a transmission line.

along the imaginary axis of an impedance plot. The second term is a circle in the complex plane. Normalizing to the characteristic impedance of the input transmission line, Z_0 (50 ohms in all of the present work), and separating the second term into real and imaginary parts gives

$$\frac{Z - jX_1}{Z_0} = \frac{R' + jX'}{Z_0} = (\omega^2 M^2/RZ_0)(1-j2Q_0\delta)/(1+4Q_0^2\delta^2) \qquad (27)$$

where $X_1 = \omega L_1$, and $R' + jX'$ is the impedance of the transformed parallel resonator shown in figure 20c.

The ratio X'/R' is $-2Q_0\delta$ from equation (27) and is the tangent of the angle θ_i of the ith impedance point of the impedance circle plotted in the rectangular impedance plane (fig. 21). θ_i is measured from the real axis to the radius vector from R = 0 to the ith point. From this we find

$$X'/R' = \tan\theta_i = 2Q_0(\omega_i-\omega_0)/\omega_i, \qquad (28)$$

which shows that frequency displacements from the point of maximum R on the real axis are proportional to $\pm \tan\theta_i$, assuming high Q. This fact from equation (28) permits accurate nonlinear interpolation of frequency around the circle. In figure 21 for example, from θ_1 and θ_2 and the corresponding frequencies, we find that a difference of tan θ of 1 between two impedance points corresponds to a frequency shift of 0.186 MHz. Then the frequencies at $R' = \pm X'$, $\theta_i = \pm 45°$, may be found and from equation (28)

$$Q_0 = 0.5\ \omega_0/(\omega_0-\omega_{45°}), \qquad (29)$$

which gives a Q for this case of 392.

The Q may be found from any two points on the circle plot using a difference formula from equation (23)

$$Q_0 = 0.5\ (\omega_1 \tan\theta_1-\omega_2 \tan\theta_2)/(\omega_1-\omega_2), \qquad (30)$$

where points 1 and 2 would usually be chosen near the ± 45° points.

Having fitted the circle to the measured data, the resistance R_0' at $X = 0$ may be found, and Q_0 is proportional to this R_0', from equation (26).

E. ANTENNA EFFICIENCY

Antenna efficiency is defined as the ratio of power radiated to the total power delivered to the antenna, equations (22) and (23). Two ways to measure efficiency are as follows:

1. Measure the power to the antenna, the antenna gain pattern, and the resulting field strength in the air, and attribute any discrepancy to inefficiency, i.e., ohmic losses [20].
2. Measure the resistance of the antenna, or its Q, when the antenna is radiating in the open and when it is enclosed in a small metallic enclosure which prevents all radiation [11]. Efficiency is obtained from the equation,

$$J = 1 - R_{open}/R_{enclosed}, \tag{31}$$

where the representation is a parallel resonant circuit. From equation (26) one finds

$$J = 1 - Q_{open}/Q_{enclosed}. \tag{32}$$

The resistances in equation (31) are each evaluated at resonance.

Efficiency was measured by the second method. The network analyzer was used to measure the impedance of the antennas near resonance, first when the antenna was radiating into the anechoic chamber, and second when the antenna was enclosed in Wheeler's so-called radiansphere [11], which for this work was a closed circular cylinder of copper, 0.6 m in diameter and 0.6 m long. These dimensions, for f = 145 MHz, satisfy the criterion that the spherical enclosure radius shall be less than the wavelength divided by 2π.

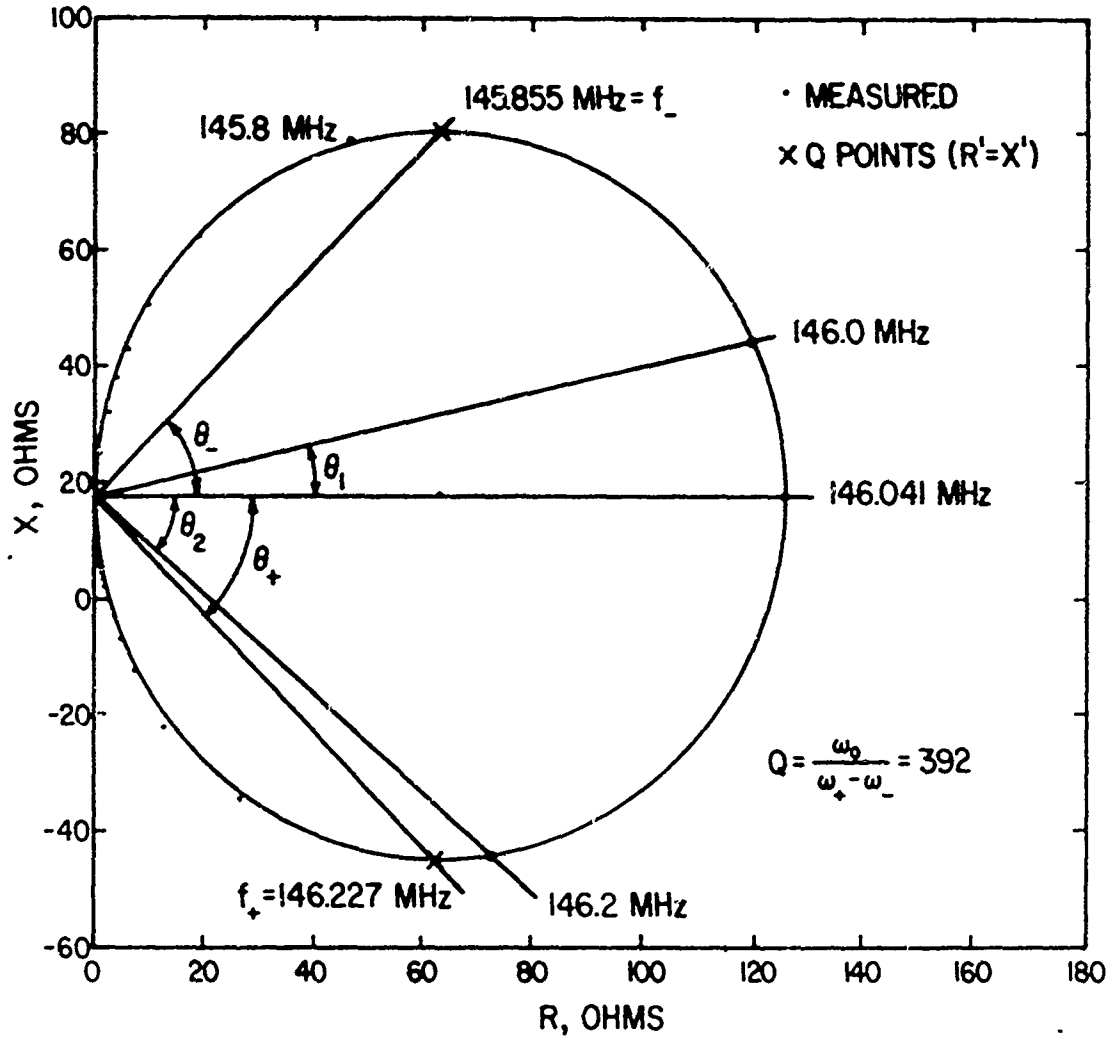

Figure 21. Q analysis, antenna enclosed in a box.

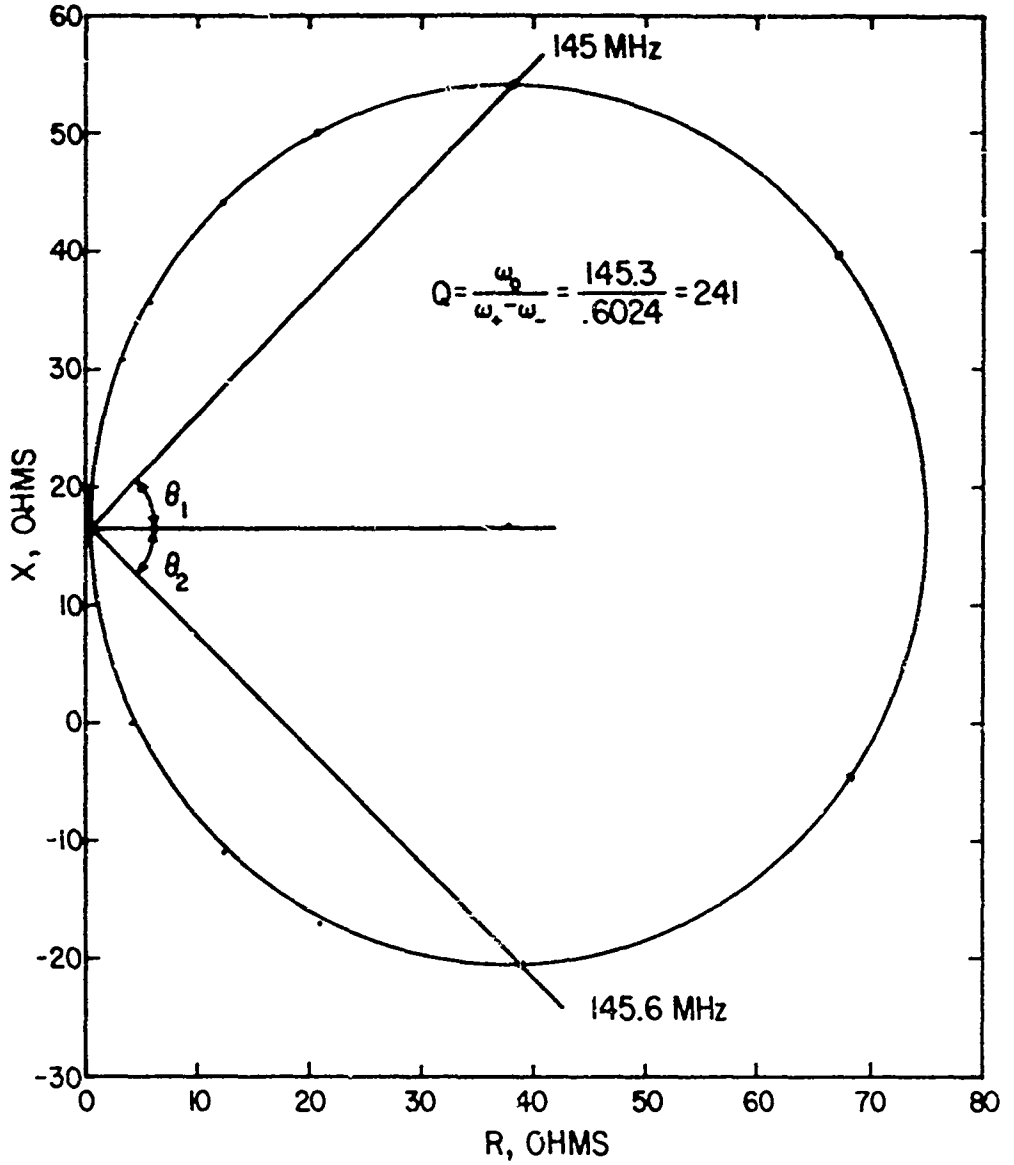

Figure 22. Same as Figure 21 but antenna radiating.

Figures 21 and 22 show the circular plots of X versus R in the rectangular impedance plane, for the enclosed and radiating conditions respectively. The Q is 392 enclosed and 235 when radiating, from which in equation (31), E = 0.4, The resistances, R_0' in the plots, are 125 and 75 respectively from which in equation (32), E = 0.4. A similar analysis was made of impedance data for five of the resonant antennas. The results are given in table 4.

The efficiencies obtained by this method are quite high. The accuracy of the method was not investigated; however, the results appear to be reasonable, and the network analyzer data certainly indicates a very definite increase in the Q when the antenna is enclosed.

Theoretical estimation of the efficiencies is of interest, and may be based on the estimated radiation and ohmic resistances of the antennas. The radiation resistances of antennas that are small compared to the wavelength may be obtained from straightforward analysis [12]. The equations are

$$R = 20\ (\pi\ell/\lambda)^2, \text{ dipole in free space}$$

$$R = 40\ (\pi\ell/\lambda)^2, \text{ monopole on a ground plane}$$

$$R = 20\ \pi^6 N^2 (D/\lambda)^4, \text{ loop in free space}$$

where ℓ is the length of the dipole or monopole, D is the diameter of the loop, λ is the wavelength, and N is the number of turns. For example at 145 MHz, for a 10 cm dipole and a 10 cm diameter one-turn loop we find

$$R = 0.5 \text{ ohm, dipole}$$

$$R = 0.11 \text{ ohm, loop.}$$

Ohmic loss must be kept small in order to obtain useful efficiencies.

Table 4. Q and maximum R', and the efficiencies calculated from the Q's and R's.

Antenna Designation	Q_{open}	$Q_{in\ cav.}$	R'_{open}	$R'_{in\ cav.}$	J(R)	J(Q)
A8	78.9	337	145	615	0.77	0.76
C4	40.6	734	631	12120	0.948	0.945
B3	70	81	2780	3350	0.17	0.14
D3	234	392	75	125	0.4	0.4
D5	37.6	2279	96	7600	0.987	0.983

Theoretical estimates of the efficiency will be given for comparison with the measurements in table 4. Consider the antenna D5, which, for purposes described later, has a coil diameter and spacing calculated to give approximately the same radiation resistance from its electric dipole moment and from its magnetic dipole moment. Using the skin depth of copper at 145 MHz, 0.0055 mm, and the dimensions in figure 19, the ohmic resistance of the full length coil is 0.16 ohms. Using sine squared current dependence on length only half of this, or 0.08 ohms, is effective. From equations (33) radiation resistances are 0.44 ohms for the magnetic dipole component and 0.32 ohms for the electric dipole component. The predicted efficiency is then

$$J = 1 - 0.08/(0.08+0.44+0.32) = 0.90,$$

which is less than the value for D5 by the radiansphere method, table 4. There is, however, at least qualitative agreement on the high efficiency.

This sort of estimate of the resistances was made for six of the antennas. The results are given in table 5, and compared with the measured values. It would appear that efficiencies can be estimated to within approximately 3 dB.

F. COUPLING COEFFICIENTS, THEORY, AND EXPERIMENTS FOR ONE ANTENNA

The coupling coefficient of a one-port resonator to a transmission line has been defined [10] as

$$\beta = (\omega M)^2/Z_0 R \tag{34}$$

which is the first term in the numerator of equation (27). β is the ratio of coupled in resistance from the line $(\omega M)^2/Z_0$

Table 5. Estimated ohmic resistance, R_{cu}, and radiation resistances, R_r and consequent estimated efficiency.

Antenna	R_r	R_{cu}	J, Estim.	J, Meas.
A8	1.5	0.27	0.85	0.76
C4	1.5	0.13	0.92	0.95
B3	0.5	1.5[a]	0.25	0.14
B4	0.27	0.21	0.56	
D3	0.11	0.03	0.78	0.4
D5	0.76	0.08	0.90	0.98

(a) The magnetic loss tangent of the ferrite was 0.011; the electric was 0.014.

to the resonator resistance R, and R is composed of two resistances in series

$$R = R_r + R_{cu}, \tag{35}$$

where R_r is radiation resistance and R_{cu} is ohmic resistance. R_{cu} includes ohmic losses in conductors, magnetic losses in magnetic cores, and dielectric losses in the dielectrics including encapsulation, and in the earth when buried, due to near field interaction (see section 6 and figure 11 of reference [1]). The coupled-in resistance is proportional to the mutual inductance squared represented in figure 20b. In the present antennas the larger the link or the higher the tap point from the base, the larger the mutual M. The resonator is overcoupled, critically coupled, undercoupled accordingly as β is greater than, equal to, less than 1. The mismatch reflection of the resonator (antenna) is a function of $R' + jX'$. If ωL_1 is suitably annulled, usually by a series capacitor for link coupling, then the reflection coefficient at resonance ($\delta = 0$ in equation (27)) is

$$|\Gamma_{res}| = (1-\beta)/(1+\beta), \tag{36}$$

which is zero when $\beta = 1$. This means that the antenna accepts maximum power from the line when it is critically coupled, provided $j\omega L_1$ has been annulled.

In general the expected qualitative relationship between input impedance and the size of the coupling link occurs. Figures 23 to 33 are Smith chart impedance plots of the type of network analyzer impedance measurements previously discussed.

The results of adjusting the coupling coefficient are illustrated by figures 23 to 25, and a change due to burial is shown by figure 27. In figure 23 the height, d, of the tap (shown in fig. 17) is 6.7 cm and the input resistance near resonance is some 210 ohms. When d = 4.5 cm the input resistance is 72 ohms (fig. 24), and when d = 2.5 cm (fig. 25) the resistance near resonance is approximately 30 ohms. In figure 26 the

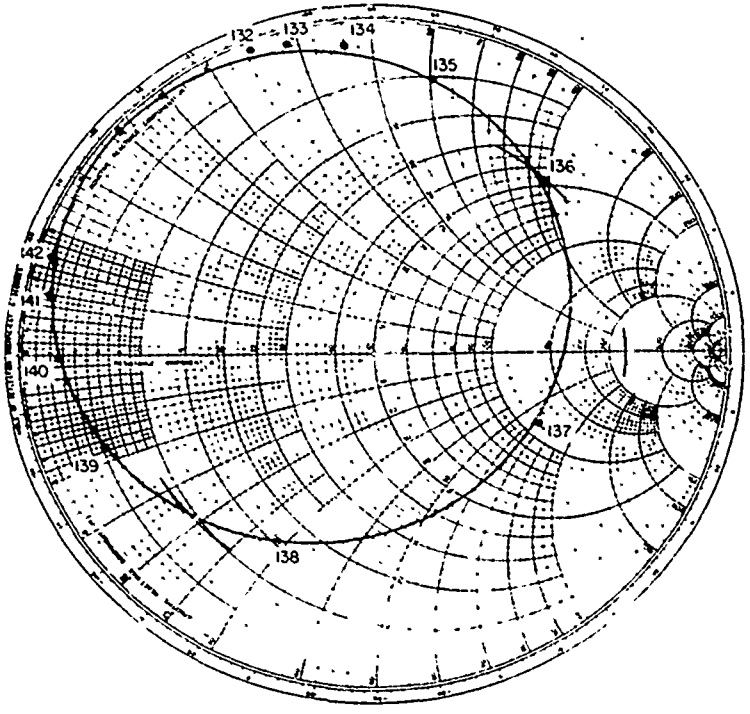

Figure 23. Impedance circle, D3-2 with d = 6.7 cm.

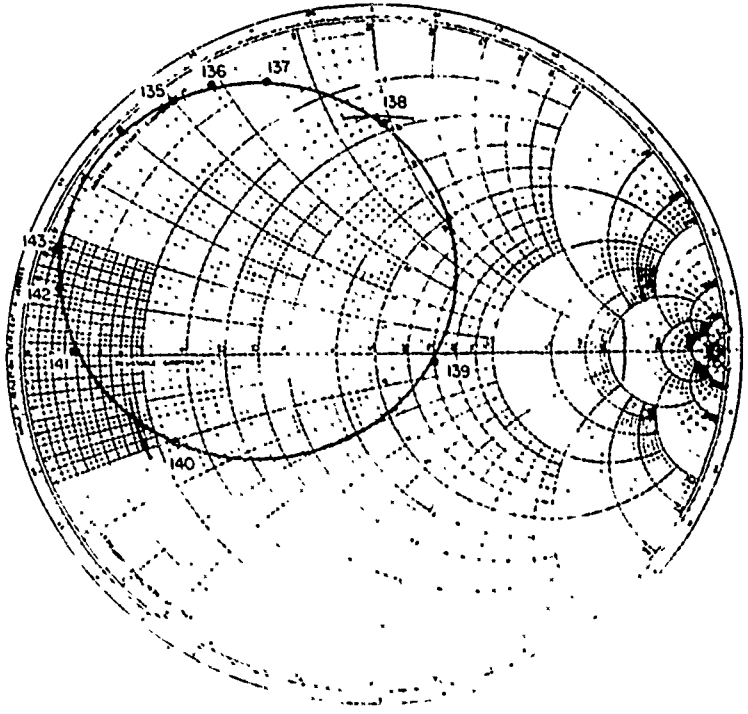

Figure 24. D3-4, d = 4.5 cm.

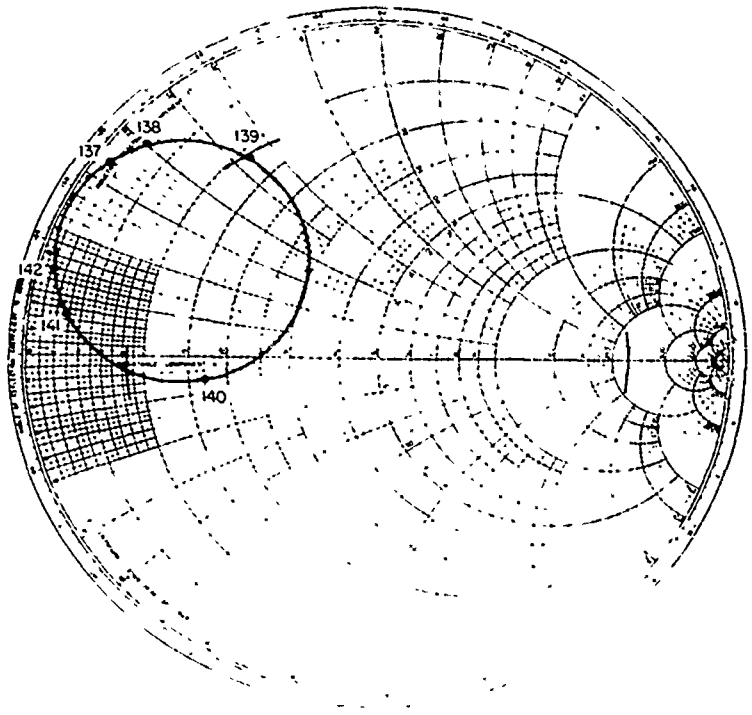

Figure 25. D3-6, d = 2.5 cm.

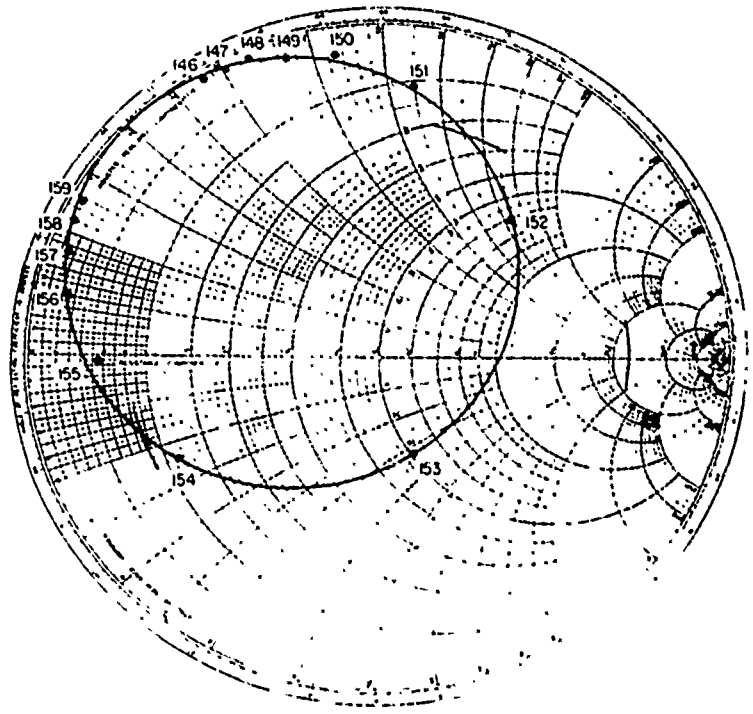

Figure 26. D3-8, d = 4.5 cm and soldered.

link was returned to approximately 4.5 cm and R was 200 ohms. The antenna was then "buried" by putting it in a hole in a concrete cylinder in the anechoic room, which adds to R through the dielectric losses in R_{cu} of equations (35), which brings the antenna nearer to critical coupling as shown in figure 27. If the concrete were more lossy the antenna would probably become undercoupled.

This work indicates that the coupling and impedance dependence on the geometry of the link and the dependence on near field dielectric losses behave qualitatively as would be expected from the theory, equation (34).

G. COUPLING, AND RADIATION RESISTANCE DISCUSSION OF ALL ANTENNAS

The impedance measurements of six of the antennas detailed in figures 13 to 19 are shown in figures 28 to 33. These measurements were made prior to making field tests discussed in figure 35 below. The impedances will be individually discussed.

The impedance plot (fig. 28) versus frequency for antenna A8 shows undercoupling, R' $\sim$ 30 ohms, and lack of capacitance. The diameter of the input link should be approximately 1.2" (3 cm). Also a small capacitor such as that in figure 14 should be in series with the link.

This antenna probably acts as an asymmetrically fed dipole, length 18 cm, radiation resistance 1.5 ohms.

The impedance of C4 (fig. 29) is too capacitive. The input capacitor should be slightly reduced. The tap at 7/8 turn gives approximately critical coupling. The radiation resistance is similar to that of A8.

The impedance of B3 is nearly 50 ohms at 146 MHz (fig. 30). The dipole length, 10 cm, gives 0.5 ohms for R_r.

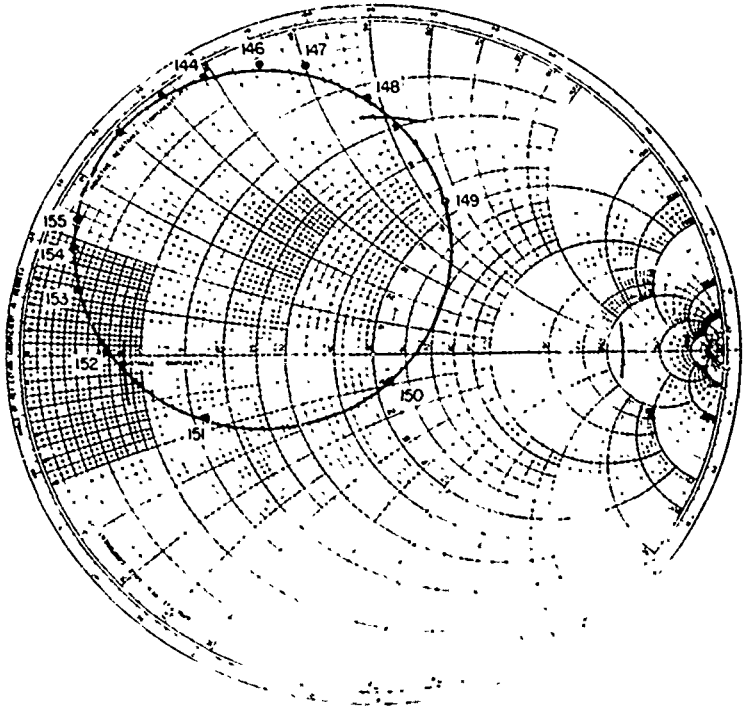

Figure 27. D3-8 buried in concrete with loss tan = 0.01.

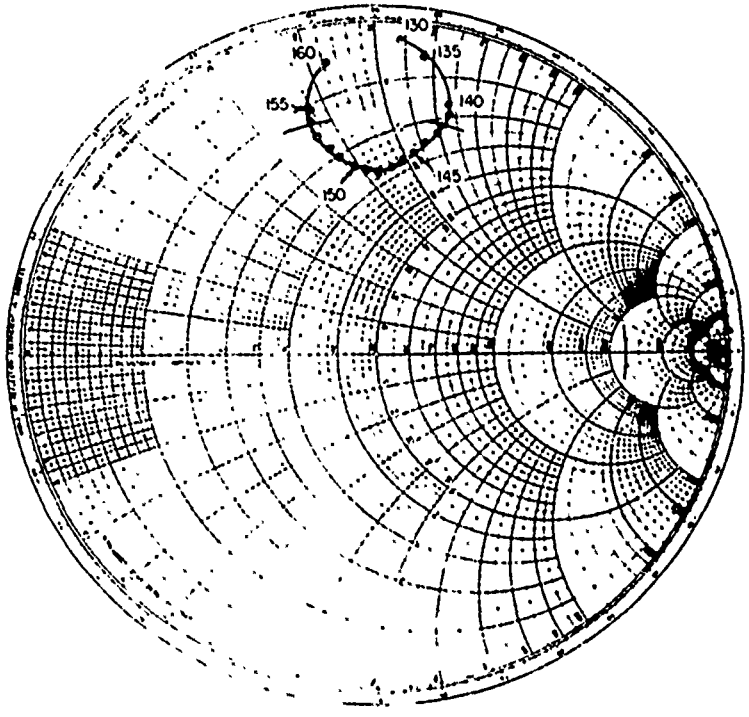

Figure 28. Impedance of A8 in anechoic room.

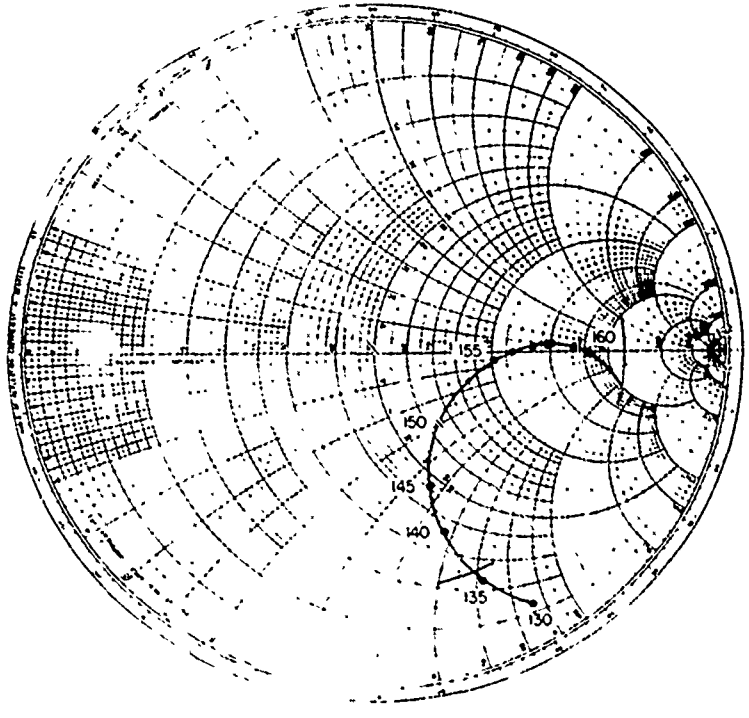

Figure 29. C4 in anechoic room.

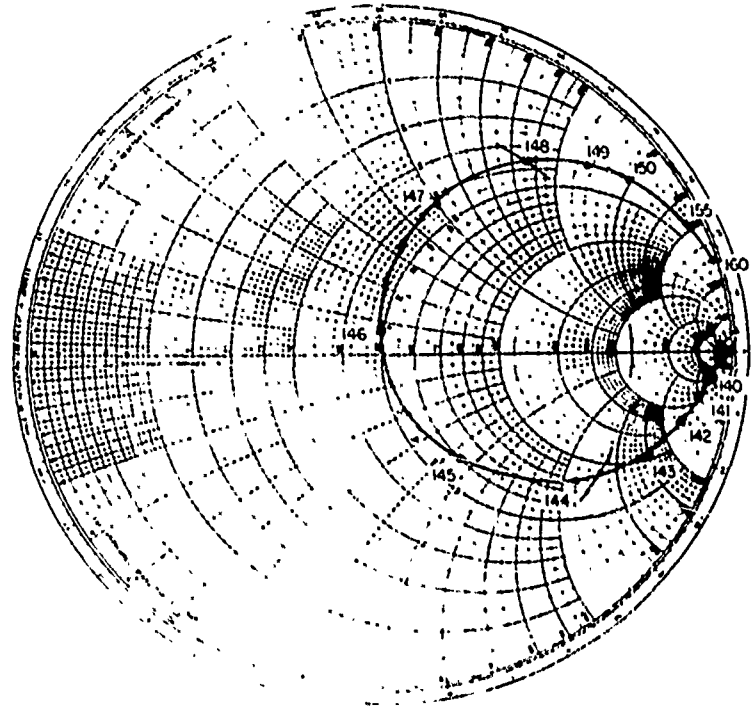

Figure 30. B3 in anechoic room.

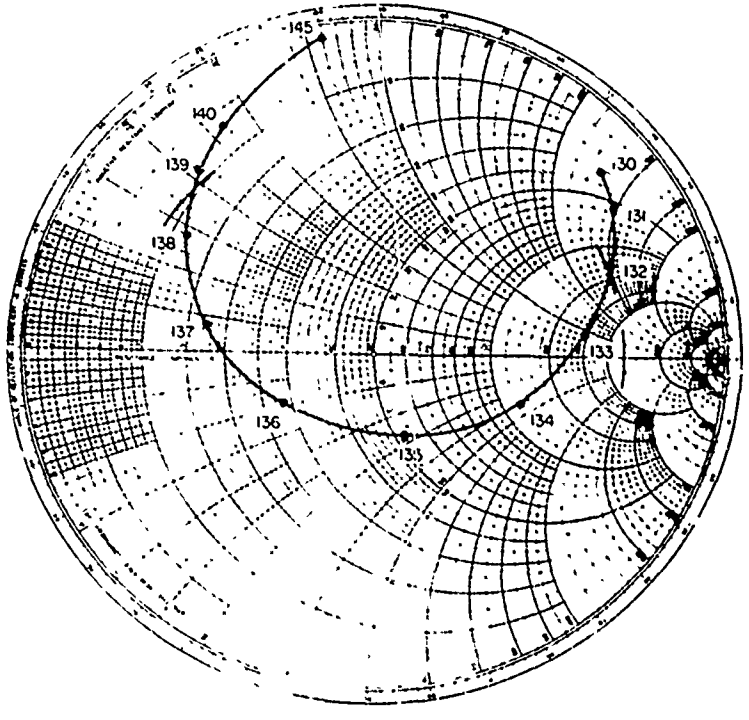

Figure 31. B4 in anechoic room.

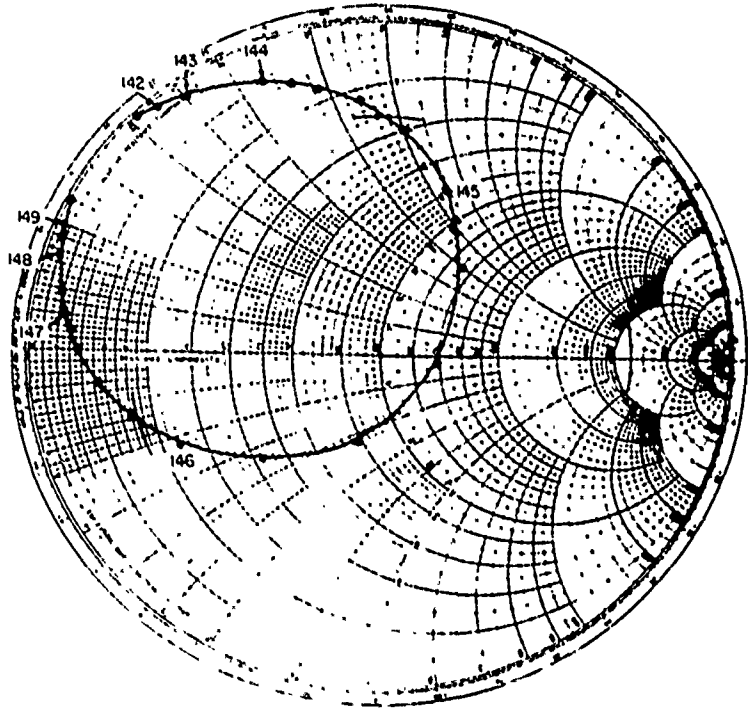

Figure 32. D3 in anechoic room.

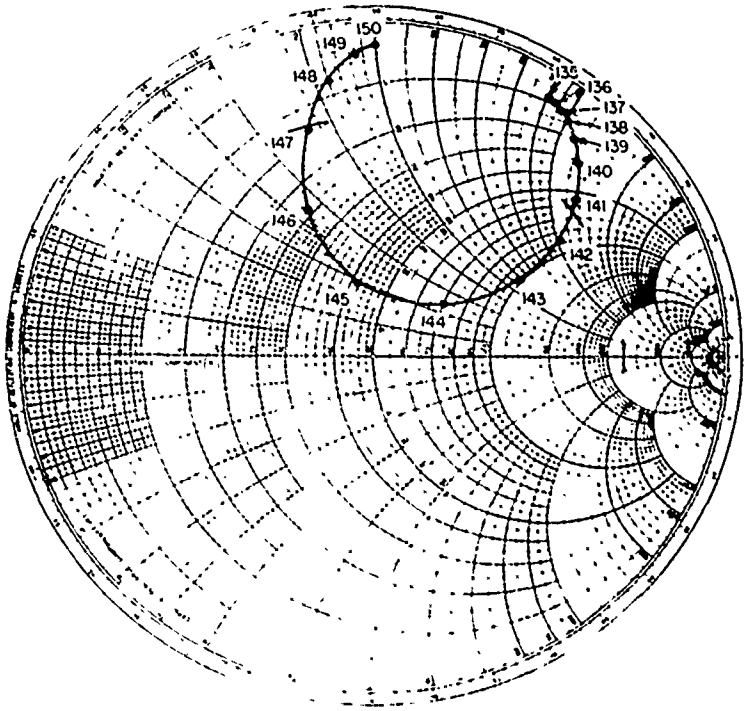

Figure 33. D5 in anechoic room.

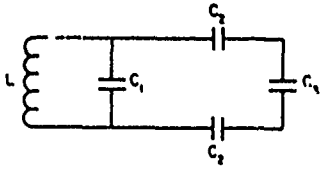

Figure 34. Circuit for analyzing interaction with burial medium.

The impedance plot of B4 (fig. 31) attains its bandwidth by leaving the input link inductive so that the curve is rather parallel to the real axis. R_r is of the order of 0.3 ohms for the 7.6 cm length coil.

The impedance plot for D3 is shown in figure 32. The coupling is correct for burial in low loss ground. The radiation resistance R_r of this loop is very low 0.11 ohms; however, the resistance R_{cu} is also low. Furthermore, a small loop has much smaller interaction with the burial medium than does an electric dipole. Therefore, the small loop probably maintains its efficiency after burial better than electric dipoles do.

The impedance of antenna D5 (fig. 33) is inductive; some input series capacitance is needed, which would improve the bandwidth as well as the impedance match. The two radiation resistances of D5 are discussed in section 4E.

The coupling development may be summarized by stating that automatic network analyzer data plotted on a Smith chart is extremely valuable in adjusting the coupling. Funds did not permit optimization of all the antennas, but the methods are rather straightforward and desirable modifications have been pointed out.

H. INTERACTION WITH THE BURIAL MEDIUM

The near electric field of the antenna interacts with the complex permittivity of the surrounding medium. As a result, the resonant frequency is lowered; the apparent ohmic loss of the antenna increases; and the radiation resistance decreases, which lowers the efficiency.

Figure 34 shows a circuit that we have used for analysis of the above-mentioned dielectric effects. It is assumed, a) that C_1 arises from the electric field that does not fringe into the burial medium; b) that C_3 arises from the electric

field in the burial medium; and c) that C_2 arises from electric field lines within the encapsulation that, in their continuations, fringe out into the burial medium and contribute to C_3.

The equation for the frequency of resonance ω_i in terms of the circuit elements and the permittivity of the burial medium, ε_i', where i denotes the ith experiment, is

$$\omega_i^{-2} = LC_1(1+C_2C_3\varepsilon_i'/(C_1(C_2+2C_3\varepsilon_i'))). \qquad (37)$$

Of the four unknowns in equation (37), three combinations, viz., LC_1, C_2/C_1, and C_3/C_1, were evaluated from the measured frequencies of resonance in three burial media, namely, air, dry sand, and concrete, with relative permittivities of 1, 2.85, and 6.5 respectively. Three antennas were so measured (table 6). The unknowns were evaluated for two of the antennas, in the third case the iterative solution employed did not converge. From the results the resonant frequencies are predicted for permittivities of 8 and 15.

The minimal encapsulation used (12.7 cm diameter plastic cover) does not provide sufficient isolation of the electric dipole antennas from the burial medium. The isolation is marginal even for the loop, D3. It will be necessary to allow a larger encapsulation; the required size was not determined; more research is needed.

I. BANDWIDTH IMPROVEMENT

Attaining required bandwidth in a resonant antenna is a research problem. Bandwidth may be increased by making longer dipoles, thus increasing the radiation resistance, and perhaps by so-called active antenna techniques [13,14]. (These two references refer to many papers on miniature and active antennas.)

Table 6. Measured frequencies of antennas buried in air, sand, and concrete; evaluation of C_2/C_1 and C_3/C_1 and prediction of resonant frequency for $\varepsilon' = 8$ and 15. Frequencies are in MHz.

Antenna	Meas. Freq. in the three Media	C_2/C_1	C_3/C_1	Calculated Freq. $\varepsilon' = 8$	Calculated Freq. $\varepsilon' = 15$
B4	150.9 133.5 128.5				
D3	167.35 165.49 163.35	0.29	0.02	162.8	161.2
D5	150.8 138.14 133.16	3.53	2.39	132.4	130.7

Small antennas have very low resistances, see table 5. Resonating them provided a way of raising the impedance for more convenient matching to a generator. Active antenna techniques provide another method of impedance matching, and at the same time usually a broadband characteristic can be obtained. Application of active antenna techniques was not made in the present research. Attention was confined to resonant techniques.

The bandwidths were measured by means of the impedance plots on Smith charts. Circular arcs representing a VSWR of 6:1 are drawn on the chart. The portion of the measured antenna impedance curve that has less than 6:1 VSWR is useful and represents the bandwidth (see figs. 28 to 33). The measured bandwidths of the antennas before modification are given in table 7.

Section 4H showed that the small loop, D3, exhibits the least interaction with the medium, which was a useful development. However, table 7 shows that D3 has a narrow bandwidth, which has some obvious disadvantages:

1. The bandwidth may be insufficient for the communications system; a spread spectrum system with 10 MHz bandwidth is a possibility.
2. The frequency shift due to burial, although small, is larger than the bandwidth, for a permittivity of the burial medium greater than approximately 2. This problem may be overcome by a larger encapsulation.

J. ADDITIONAL MODIFICATION OF ANTENNAS; RESULTING BANDWIDTH AND INTERACTION WITH MEDIA

Last-minute modifications of the antennas were performed with the purpose of making the frequency when buried nearer to 145 MHz, or improving the coupling, e.g., by the experiments on D3 described in part F. The changes were not always beneficial but are of interest especially for bandwidth and frequency shift purposes. The changes and measured characteristics are listed in table 8.

Table 7. Measured bandwidths of the antenna in the anechoic chamber, defined as the frequency region where more than half of the power is accepted from the transmission line, i.e., VSWR less than 6:1.

Antenna	Bandwidth, MHz
A8	11.6
C4	27
B3	4.4
B4	6.7
D3	1.5
D5	5.9

Table 8. Characteristics of the changed antennas

Antenna	Frequency (MHz) in air	Frequency (MHz) in concrete	Bandwidth[b] (MHz) in air	Bandwidth[b] (MHz) in concrete	Changes Made
A8-2	164	149[a]	20	8	Coil=3.25 turns. Coupling tap at ½ turn.
C4-2	147	135[a]	47	13	Coil=2.5 turns, 9.4 cm high. Coupling tap at 3/4 turn.
B3-2	150	139	2.8	2.6	Capac plate now circular. Coupling link, approximately as in D5.
B4-2	152	129	5.5	4.9	Coil stretched out=6.3 cm. Coupling, no change.
D3-8	153	150	2.9	3.5	Capacitor spaced 0.25 cm. Input link 0.94 cm gap and 4.6 cm to the short.
D5-2	153	148	1.4	0.8	Coil=2.8 turns with 1.6 cm turn spacing. Coupling link centered on coil, coil rotated 90° around its axis.
D6	149	138	0.8	1.1	Similar to D5, but with 8.9 cm diameter capacitor plates on the ends. Coupling link similar to that of D5.

(a) Frequency when set at interface, not buried, A8-2 = 163 MHz, and C4-2 = 146 MHz.

(b) Bandwidth is obtained from Smith chart impedance plots, and is defined as the frequency region in which the VSWR is less than 6:1.

Usually the bandwidth decreased on burial in concrete, in the anechoic room. From the impedance plots (not shown) it appears that only antenna D3-8 is suitably coupled. The others are too inductive, and overcoupled or undercoupled. Antenna C4-2 is incorrectly coupled but does have very large bandwidth. The results indicate that trial and error experiments on impedance and coupling are usually required in order to approach an optimum.

K. CONCLUSIONS FOR SECTION 4

Section 4 contains construction details for six resonant antennas, and a detailed account of using impedance data to study Q, coupling, efficiency, bandwidth, and interaction with the burial medium. Theoretical circuit analysis of resonant antennas has been described and applied to the mentioned charactersitics.

An outstanding conclusion from this work arises from a synthesis of the findings. From theory and by inspection of the results in tables 6, 7 and 8, we make the hypothesis that the frequency shift due to burial is approximately proportional to the bandwidth. For example a long dipole has more stray field, giving more C_3 in the circuit representation (fig. 34), and because of its length, more radiation resistance. Thus the Q will decrease and the bandwidth will increase, which is very desirable; but the frequency shift due to more stray field is larger, which is undesirable. Table 8 shows that in most cases the shift in the resonant frequency due to burial in concrete, $\varepsilon' = 6.5$, is greater than half the bandwidth, which means that the oscillator and antennas must be tuned beforehand in anticipation of the burial. According to equation (37) and the predictions in table 6 the frequency decrease saturates

as ε' increases. This fact might be useful in offsetting the frequency of the generator and the antenna in air in anticipation of the shift of resonance upon burial.

Footnote (a) of table 8 shows that the so-called monopole antennas, A8 and C4, shift frequency only by 1 MHz when the top of the copper base is flush with the interface. Unfortunately, the frequency shift for partial burial (antenna top flush with the surface) was not obtained. In view of the suggestion in section 3G, to partially bury the monopoles, flush with the surface, it would be important to obtain a curve of frequency shift as a function of the penetration through the interface.

Active antenna techniques versus resonance techniques should also be investigated.

5. FIELD TESTS OF BURIED ANTENNAS

A. INTRODUCTION

Some field test results have been presented already in section 3. The important remaining field tests indicate performances of candidate antennas, which for reasons stated are small antennas.

If the theory is obeyed, as was concluded in section 3, and if the efficiency is known from the various methods in section 4, then comparison measurements as presented here are unnecessary; however, measurements were made and are believed to be worthwhile for verification. Also, the theory of a partially buried finite dipole was not treated; therefore, experiments are necessary for low-profile vertical dipoles.

B. THEORETICAL AND PRACTICAL CONSIDERATIONS

The space wave field depends on theoretical factors which are understood. The field after burial is predicted to be

$$E = E_f \; I \; D \; P \; J^{\frac{1}{2}}, \tag{38}$$

where E_f is the free space inverse distance field of equation (6), I is the interface loss of figures 2 and 5; D is the depth loss of equations (1) and figure 3; P is the underground pattern factor of figure 4 including in addition cos ϕ or sin ϕ for angles other than broadside and end fire, and J is the efficiency from equation (23).

The TM wave of the vertical electric dipole suffers considerable pattern loss P unless the dipole is "low profile," not fully buried.

The TM wave broadside from the horizontal magnetic dipole is theoretically the strongest possible wave. The pattern factor P is 1. The efficiency is least degraded by burial because a small loop has small near electric fields to interact with the losses of the burial medium. However, as seen in table 4 the ohmic efficiency of the 10 cm diameter loop (D3) is somewhat low; a 13 cm diameter would probably reduce the ohmic inefficiency loss to less than 1 dB loss.

The small loop is also attractive as a low-profile antenna, not fully buried. It does not, however, furnish the convenient 360° azimuthal coverage of the low-profile vertical dipole; crossed loops for circular polarization on the vertical axis would be required, and there is a loss of 3 dB compared to the vertical dipole because approximately half the energy of a horizontal dipole goes into TE waves.

The antenna D5 was designed with a diameter and pitch to give equal radiations from the electric and magnetic dipole moments [15]; furthermore, the theory shows that these two radiations are 90° out of phase, giving circular polarization. Thus, considering the broadside and end fire TM waves, there is 360° azimuthal coverage with TM waves from the buried horizontal electric and magnetic dipoles.

C. FIELD SITE PERFORMANCE OF SMALL ANTENNAS

The measuring arrangement is that indicated in figure 6. The field site is on the NBS grounds and is not as smooth as the previously mentioned alfalfa field. Burial is accomplished by placing concrete rings in the ground with outer diameter 30.5 cm and inner diameter 13 cm to accept each 12.7 cm diameter candidate antenna. Concrete disks are put on top of the antenna after it is set down in the hole. By this method, to a good approximation, all antennas are buried under the same medium of known dielectric constant.

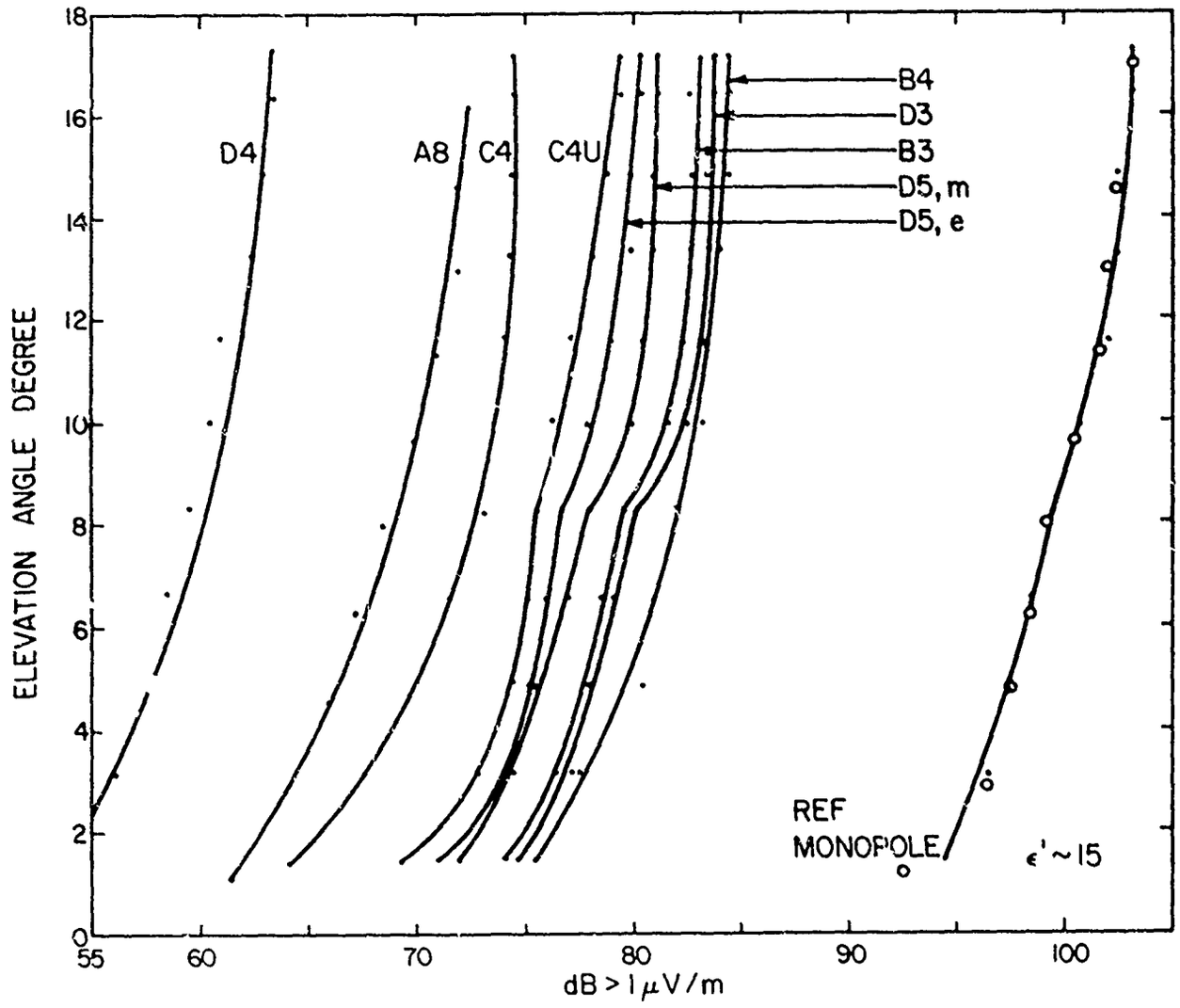

Figure 35. Field measured at R = 30.5 m; P_a = 1 w to the buried antenna.

The concrete was made from a 94% aluminum oxide cement. It was assumed to have a relative dielectric constant of 6.5 and a loss tangent of approximately 0.008, since it was cured at elevated temperature, 125°C, as recommended in [8].

Figure 35 shows the received field strength in dB greater than 1 microvolt per meter at 30.5 m horizontal distance, normalized to 1 W power input into the antenna, for several antennas. The field strengths were obtained from the received voltage, taking into account transmitted power and receiving conversion factors as outlined in section 3D and 3E. The length, u, of the transmitter cable was 10.7 m. In addition, a small correction was estimated to allow for the change in efficiency of the antenna due to the lower resonant frequency (below 145 MHz) when buried. Table 9 lists the test frequency and the conversion factors just mentioned. Bends in many curves of figure 35 are similar to bends observed in reference [8], which were due to a mismatch between the concrete and the earth.

The results show that antenna B4, a HED, furnishes the strongest signal, by a small margin. The loop D3 is slightly weaker, presumably due to inefficiency, because its radiation resistance is only 0.11 ohm. The loop needs to be larger.

The circularly polarized design D5 is a very good antenna. For performance comparisons 3 dB should be added to both measured fields in order to compare on the same power basis with B3, B4, and D3. This is true because D5 consists in effect of two crossed dipoles. B3, B4 and D3 would have to be fabricated as crossed dipoles fed 90° out of phase to give the same field coverage as D5, and would lose 3 dB in the process.

It will be noted that this group of horizontal dipoles, all of similar performances, (converting to 360° coverage) is about 20 dB weaker than the reference monopole. This loss is unavoidable for a horizontal electric dipole. The theoretical losses relative to isotropic may be itemized as follows,

Table 9. Conversion factors to obtain field strength normalized to 1 W power into the antenna, and correction for the lower efficiency due to the frequency being less than 145 MHz.

Antenna	Test Freq. MHz	Conversion to Field and 1 W Normaliz., dB	Correction[c] for Freq. Effect on Efficiency, +dB
A8	130.3	-1.37	0.06
C4	111.6	-2.05	0.34
C4,u[a]	116.5	-2.2	0.34
B3	128.1	-1.2	0.9
B4	113.1	-2.1	1.0
D3	142.9	+1.0	0.14
D4	146.5	+1.1	--
D5,e[b]	117.1	-2.2	0.05
D5,m[b]	116.7	-2.2	0.11
Monopole	145	+0.1	--

(a) Antenna buried about 5 cm; other burials were 10 to 20 cm.

(b) The letters e and m signify the electric and magnetic dipole radiations of the coil, respectively.

(c) Efficiency $J = R_r/(R_r+R_{cu})$; R_r is proportional to f^2 for electric dipoles and f^4 for magnetic dipoles.

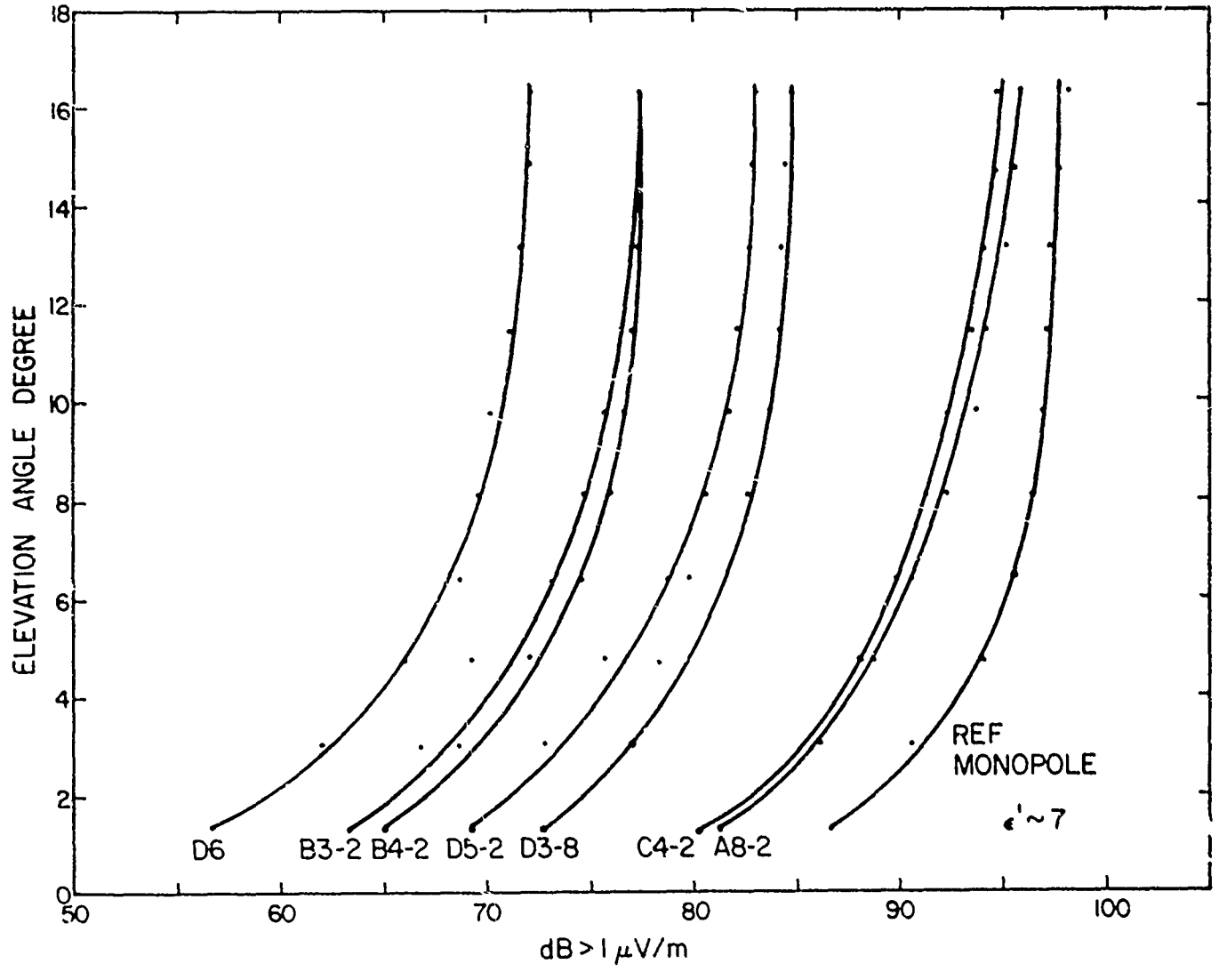

Figure 36. Same as Figure 35 but antennas modified.

at 10° elevation, and dielectric constant of the burial medium = 6.5:

a.	Interface loss, I,	14 dB
b.	Depth loss, D,	0.2 dB
c.	Pattern factor, P	0.3 dB
d.	Circular polarization power loss	3 dB
e.	Efficiency, J, ∿ 1 to 3 dB	

Total Loss, Relative to Isotropic, 18.5 to 20.5 dB. Some of this loss might be avoidable with D3 as a low-profile partially buried antenna.

The reference antenna has approximately 0 dB gain with respect to an isotropic emitter at 10° elevation. The HED system with 360° azimuthal coverage is approximately 20 dB weaker than the monopole experimentally; thus the experiment is in good agreement with the above theoretical estimate.

Figure 36 shows electric field strength patterns, measured in the same way as in figure 35, but after the candidate antennas were modified as indicated in table 8.

The D3 antenna, with nearly optimum coupling and the frequency increased by 5 percent, now gives more signal than B3 and B4. Surprisingly D3 is only 13 dB weaker than the reference monopole (16 dB weaker, if circular polarization coverage is added). However, the reference monopole is approximately 4 dB weaker than in figure 35, presumably because the ground was dry for figure 36 and wet for figure 35. D3 on an absolute basis (relative to isotropic) is approximately 1 dB better than in figure 35. At any rate D3 is doing as well as can be expected for an antenna buried in a medium with $\varepsilon' \sim 6.5$.

Antenna D5-2 was modified incorrectly and consequently it lost much of its electric dipole strength, but the magnetic dipole component is still very good.

Antennas B3-2 and B4-2, as modified, and D6 are in need of further development.

The vertical dipoles A8-2 and C4-2 were not buried; the top of the base was at the interface. The resonant frequencies were only lowered 1 MHz by this partial "burial." These antennas furnish 360° azimuthal coverage. If the low profiles (7 and 10 cm) are acceptable for concealment, then these are certainly convenient and useful antennas. They are easy to fabricate, can have a bandwidth of 10 MHz or more, and give fields about 4 dB weaker than does the reference monopole.

Figure 12 has indicated the variation of loss as a function of burial depth. However, more work of this type is desirable in order to know the effect of various parameters, such as dielectric constant and conductivity, on the curves shown in figure 12.

D. SUMMARY OF RESONANT ANTENNAS

The low-profile vertical electric dipole, VED, at the earth's surface conveniently furnishes the desired TM wave (wave with horizontal magnetic vector) in space without serious inefficiency loss or burial loss.

The profile can be flush with the interface by accepting some additional loss. The amount of this loss (fig. 12) can be reduced by a larger encapsulation diameter than the 13 cm diameter used here.

A low profile situated or a "flush" buried HMD, i.e., antenna D3, figure 17, has approximately 3 dB less gain than the VED because half of its energy goes into TE waves. It will be less convenient because crossed dipoles for circular polarization are required.

The HED either on the surface or buried will suffer the apparently unavoidable interface loss, furnishing a gain of -18 to -20 dB below that of a reference monopole on the interface, assuming a dielectric constant of 6.5.

6. PREDICTED DISTANCE OF COMMUNICATION

A. INTRODUCTION

The gain of a fully buried antenna appears to be that predicted by Sommerfeld theory [1] as given by equations (1) above. The gain of a low profile vertical dipole is approximately -4 dB relative to a high efficiency quarter wavelength monopole on a one wavelength diameter metal disk, and the latter has well known gain properties [7]. Using these facts, predictions may be made of the distance over which communications can be received from buried and low-profile antennas.

B. ASSUMED TRANSMITTER POWER AND RECEIVER CHARACTERISTICS

It will be assumed that 1 W is accepted by the buried or partially buried antenna, of which the fraction J is radiated, where J is the antenna efficiency.

The criterion for reception depends on the bandwidth, noise level, and modulation scheme. At 145 MHz the equivalent median value field strengths due to various noise sources are estimated as follows, per kHz receiver bandwidth [16]:

Urban Man-Made Noise	$\sim$ -120 dBV/m/kHz
Cosmic Noise	$\sim$ -129 dBV/m/kHz
Internal Receiver Noise	$\sim$ -138 dBV/m/kHz

The field specified for equaling internal receiver noise may be interpreted as follows: The room temperature Johnson noise of a 50 ohm resistor, approximately -151 dBV/kHz,* has been converted to equivalent field strength using the dipole conversion factor of 9.3 dB, section 3C, and a noise figure of 3.7 dB has been included, yielding -138 dBV/m/kHz. A rural environment without urban noise will be assumed.

*dBV/kHz denotes dB relative to 1 volt, per kHz bandwidth. dBV/m/kHz denotes an equivalent field in volts per meter per kHz [16].

The bandwidth of a modern receiver may reasonably be of the order of 10 to 100 kHz. Using the cosmic noise level of -129 dBV/m/kHz as a criterion for reception, the required signal electric field in the air is

-119 dBV/m, at 10 kHz bandwidth

-109 dBV/m, at 100 kHz bandwidth,

for a 1:1 signal to noise ratio, S/N.

C. GAIN PATTERN OVER A SPHERICAL EARTH

All preceding discussions of the gain pattern in the air space have been for a flat earth. Fortunately, at the angles considered, elevation angles of 1° or more, the flat earth results also apply to spherical earth propagation at UHF frequencies, provided that the elevation angle of the field pattern is measured with respect to a plane tangent to the sphere at the point where the antenna is buried [17]. Reference [17] shows that at elevation angles of 1° or more the field of a monopole or dipole located on or near the earth is nearly the same for a flat earth and for a spherical earth. The tangent plane would be somewhat spherical to allow for the earth's atmosphere, but instead we use the usual 4/3 earth's radius approximation [18]. Then the height h in feet of the new flat tangent plane is $h = R^2/2$ where R is the horizontal distance in miles from the point of tangency. The elevation angle is obtained from the height above this tangent plane.

D. FIELD STRENGTH VERSUS DISTANCE

The chosen communications model is a 1 W source driving a buried or a low-profile antenna and a receiver 50,000 feet above the spherical earth. Figure 37 shows the predicted fields versus the horizontal distance for various conditions. Only a TM wave is considered.

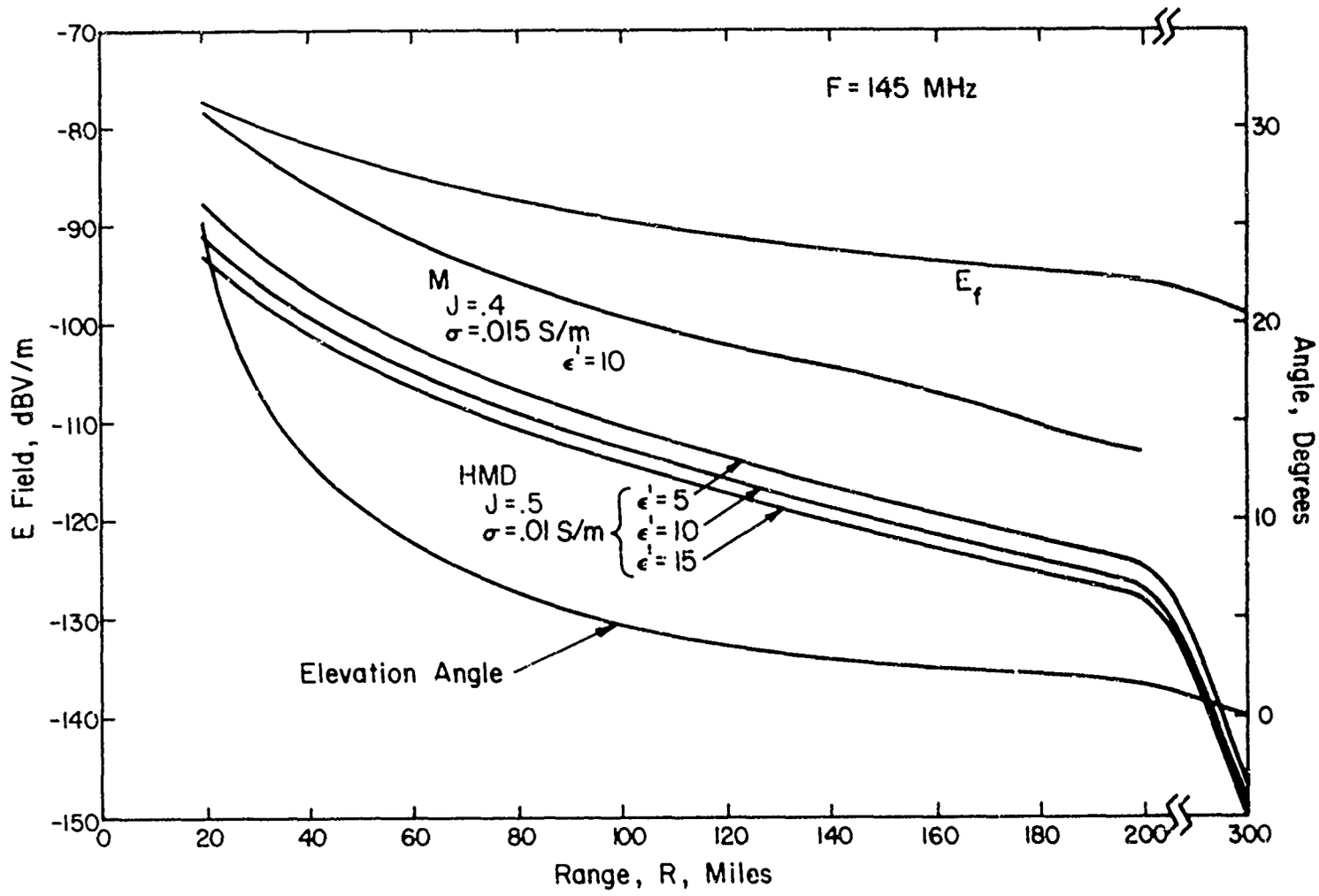

Figure 37. Field strength at 50,000 feet versus range; 1 watt source,

The curve E_f for free space is evaluated from equation (6). The elevation angle, measured as previously discussed, is indicated by another curve. The curve marked M (monopole) is evaluated from

$$E = E_f \, M \, J^{\frac{1}{2}} \tag{39}$$

where M is the vertical monopole pattern factor [7] of figure 9, and J = 0.4 to represent the 4 dB loss of the low-profile vertical dipole (fig. 36) compared to the "reference" monopole.

The group of curves with parameters $\varepsilon' = 5$, 10, and 15 is evaluated for a buried loop (HMD) using equation (38)

$$E = E_f \, I \, D \, P \, J^{\frac{1}{2}}.$$

It is assumed that P = 1 for the HMD, that D = 1 (shallow burial), and that J = 0.5. The computer routine used for figure 2 was modified to include the proper angle and range.

A field strength of -109 dBV/m, as suggested above for equaling cosmic noise in a 100 kHz bandwidth receiver, will be used as a criterion for reception. (Reference [19] in a study of spread spectrum techniques uses an ultimate receiver sensitivity of -107 dBm corresponding to -120 dBV at the receiver and -110 dBV/m field strength in the air. We have, however, used -109 dBV/m as a criterion.)

The results for the buried HMD antenna show that a field of -109 dBV/m occurs at 92 miles for $\varepsilon' = 5$, at 79 miles for $\varepsilon' = 10$, and at 72 miles for $\varepsilon' = 15$. The conductivity was 0.01 S/m throughout. The curve M for the low profile VED falls to -109 dBV/m at a range of 172 miles.

The communications range may be found for other source powers by a shift of scale of 10 dB per factor 10 in power. Also other criteria may be used for the required field strength for reception; e.g., the assumed dipole receiving antenna may be replaced by a higher gain antenna to increase R.

7. DISCUSSION AND CONCLUSIONS

Electrically small resonant dipole antennas were developed to be buried in the earth for concealment. For a buried dipole, the gain and the pattern in the upper half space are well predicted by Sommerfeld theory and also in general by physical optics methods which were developed. Experiments confirm the theoretical factors, in particular the interface loss and the pattern in space. A "reference" monopole on the surface confirmed the accuracy, ± 1 dB, of the overall measuring system, i.e., of the transmitted power and received field strength measurements.

In contrast with above-ground antenna experience, the required TM wave is not best obtained from a buried vertical dipole. Buried horizontal dipoles, either the HMD or the HED, provide stronger TM waves, but there is a sine or cosine azimuthal dependence. Coverage over 360° is provided by crossed horizontal dipole with circular polarization.

The interface loss due to burial will often be in the range of 15 to 25 dB; it increases with the dielectric constant of the ground. An additional difficulty is the shift of the resonant frequency and consequent mismatch of the antenna to the generator, resulting from burial. The resonant electric dipoles may remain matched to the generator after burial, either by adjusting for the frequency shift ahead of time, or by using a larger encapsulation to prevent interaction with the ground. The preceding statement probably also applies to resonant loops. The roughly 10 cm diameter loop investigated had a comparatively small frequency shift, table 6, but still it exceeded the bandwidth of the resonance, table 7.

In view of the above problems, methods of avoiding fully buried antenna are desirable. Convenient vertical dipoles, figures 13 and 14, may be partially buried, rising 7.5 and 10 cm

above the earth's surface respectively. The loss due to burial is then approximately 4 to 5 dB (fig. 36), and TM waves are obtained over 360° in azimuth. The frequency shift due to burial in $\varepsilon' = 6.5$ was small, 1 MHz. Theoretically, crossed HMD loops with circular polarization would also function well as a low-profile antenna. Finally, this antenna and the VED could be set flush with the surface of the ground for concealment, and with a slightly larger, 15 to 18 cm, diameter plastic cover, the loss due to burial is estimated to be only 5 to 10 dB more than for low-profile above-ground antennas.

Active antenna techniques, section 41, remain to be investigated. These techniques have been used [13] instead of resonance to match an antenna to generator. The advantage would be that the impedance match would not be lost if the system were buried.

Section 4 gives a detailed account of impedance measurements for analysis of the efficiency, bandwidth, coupling, and interaction with the burial medium.

The predicted maximum range of communication with 1 W power and a receiver at 50,000 feet altitude is 170 miles using a low-profile VED. The predicted range when the antenna is a fully buried HMD (resonant loop) is 70 to 90 miles.

According to reciprocity theory the antennas developed here for transmitting purposes will have the same burial loss and efficiency when used as receiving antennas.

It is recommended that the present research be extended to include a study of the bandwidth, frequency shift, and interface attenuation as functions of shallow burial depth (near the interface) and as functions of the size of the encapsulation. Also, the allowed dimensions for convenient tactical deployment should be redetermined with the idea of obtaining increased bandwidth by a larger structure.

The active antenna alternative should be investigated and might obviate the frequency shift and bandwidth problems encountered,

The buried HED and HMD antennas are useful assuming that the frequency shift due to burial is engineered into the design, or reduced by allowing more encapsulation. The VED antennas A8 and C4, figures 13 and 14, may be used as convenient low profile partially buried antennas.

REFERENCES

[1] Hufford, George A., UHF Propagation from Buried Antennas, U.S. ESSA Research Laboratories, ITS, ESSA Tech. Memorandum ERLTM-ITS 191, 68 pages, July 1969.

[2] Moore, R.K. and W.E. Blair, Dipole Radiation in a Conducting Half Space, NBS Journal of Research, 65D, 547-563, 1961.

[3] Banõs, A., Dipole Radiation in the Presence of a Conducting Half Space, Pergamon Press, Oxford, 1966.

[4] Biggs, A.W. and H.M. Swarm, Radiation Fields of an Inclined Electric Dipole Immersed in a Semi-Infinite Conducting Medium, IEEE Trans. Antennas & Propagation, AP-11, No. 3, 306-310, May 1963.

[5] Stratton, J.A., Electromagnetic Theory, McGraw-Hill Co., New York, 1941.

[6] Greene, F.M., NBS Field-Strength Standards and Measurements (30 Hz to 1000 MHz), Proc. IEEE, 55, 970-981, June 1967.

[7] Ma, M.T. and L.C. Walters, Power Gains for Antennas Over Lossy Plane Ground, ESSA Technical Report ERL 104-ITS 74, April 1969.

[8] Fitzgerrell, R.G., R.L. Gallawa, L.L. Haidle, A.Q. Howard, Jr. and J.E. Partch, Buried Vertically Polarized UHF Antennas, Inst. Telecom. Sci., Boulder, Colo., OT/ITS R and E Rept. 8, Nov. 1970.

[9] Cottony, H.V., Gain Pattern of Hardened Antennas Using Dipoles as Radiating Elements, Inst. Telecom. Sci., Boulder, Colo., OT/ITS R and E Rept. 20, Oct. 1971.

[10] Ginzton, E.L., Microwave Measurements, McGraw-Hill Book Co., New York, 1957.

[11] Wheeler, H.A., The Radiansphere Around a Small Antenna (see Radiation Shield), Proc. IRE, 47, 1325-1331, Aug. 1959.

[12] Schelkunoff, S.A. and H. Friis, Antennas Theory and Practice, J. Wiley and Sons, New York, 1952.

Preceding page blank

[13] Turner, E.M., A Regenerative Broadband Electrically Small Folded Dipole Antenna, Abstracts of the 22nd Annual Symposium, USAF Antenna Research and Development Program, Sponsored by AF Avionics Lab. WPAFB, and the University of Illinois, Monticello, Ill., in the session on Phased Array Techniques.

[14] Dunlavy, J.H., Jr. and B.C. Reynolds, Electrically Small Antennas, Same Conference as Reference [13], in the session on Components and Lens Techniques.

[15] Kraus, J.D., Antennas, First Edition, McGraw-Hill Co., New York, 1950 (eq. 7.4 of Section 7.4).

[16] White, Donald R.J., Handbook Series on Electromagnetic Interference, Vol. 1, Electrical Noise and Electromagnetic Interference Specifications, Don White Consultants, Germantown, Maryland, USA, 1971 (fig. 1.1).

[17] Berry, L.A. and M.E. Chrisman, Linear High Frequency Antennas Over a Finitely Conducting Spherical Earth, ESSA Technical Report, IER 8-ITSA 8, Inst. for Telecommunication Sci., Boulder, Colo., USA, Sept. 1966.

[18] Westman, H.P., Editor, Reference Data for Radio Engineers, International Telephone and Telegraph Co., New York, Fourth Edition, Chapter 24, 742, 1956.

[19] Ridings, R.V., C.R. Reeves and J.P. Aasterud, Modulation Waveform Study, RADC TR-73-77, Final Report, March 1973.

[20] IEEE Standards Committee, IEEE Test Procedure for Antennas, IEEE Trans. Antennas & Propagation, AP-13, No. 3, 437-466, May 1965.

July 1972

BIBLIOGRAPHY ON BURIED ANTENNAS

by

The NBS Electromagnetics Division Staff

The literature search activities have progressed well and the following bibliography has been developed, and used in the theoretical study, and for planning the experiments.

The Quasi-Static Fields of Dipole Antennas - Part I
Bannister, Peter R.
U.S. Navy Underwater Sound Laboratory
USL Research Report 701, Project No. 1-901-00-00
Jan. 3, 1966, 38 pages

The Near Fields of Subsurface Electric Dipole Antennas
Bannister, Peter R. and William C. Hart
U.S. Navy Underwater Sound Laboratory
USL Report No. 728
Mar. 4, 1966, 12 pages

The Electric and Magnetic Fields Near a Buried Long Horizontal Line Source
Bannister, Peter R.
U.S. Navy Underwater Sound Laboratory
USL Report No. 991
June 4, 1969, 20 pages

Input Resistances of Horizontal Electric and Vertical Magnetic Dipoles Over a Homogeneous Ground
Bhattacharyya, B. K.
IEEE Trans. Antennas & Propagation
May 1963, Vol. AP-11, No. 3, 261-266

Radiation Fields from a Horizontal Electric Dipole in a Semi-Infinite Conducting Medium
Biggs, Albert W.
IRE Trans. Antennas & Propagation
July 1962, Vol. AP-10, 358-362

Radiation Fields of an Inclined Electric Dipole Immersed in a Semi-Infinite Conducting Medium
Biggs, A. W. and H. M. Swarm
IEEE Trans. Antennas & Propagation
May 1963, Vol. AP-11, No. 3, 306-310

A Modeling Technique for Experimental Verification of Dipole Radiation in a Conducting Half Space
Blair, W. E.
U. New Mexico, Contract Nonr 2798(01)
Tech. Report EE-59
July 1962, 47 pages

Experimental Verification of Dipole Radiation in a Conducting Half-Space
Blair, W. E.
IEEE Trans. Antennas & Propagation
May 1963, Vol. AP-11, No. 3, 269-275

Radio Waves in Rock Near Overburden-Rock Interface
Carolan, J., Jr. and J. T. deBettencourt
IEEE Trans. Antennas & Propagation
May 1963, Vol. AP-11, No. 3, 336-338

Vertical Electric Dipole in a Two Conductor Region
Carolan, James F.
Air Force Cambridge Research Laboratories
(Prepared by Raytheon Co., Norwood, MA, Contract No. AF19(628)-2362, Project No. 4600, Task No. 460008)
Scientific Report No. 4
Apr. 1964, 32 pages

Current on and Input Impedance of a Cylindrical Antenna
Chen, Yung Ming and Joseph B. Keller
NBS J. Research
Jan.-Feb. 1962, Vol. 66D, No. 1, 15-21

Further HF Tests on the Wyoming Buried Dipole
Crombie, D. D.
U.S. ESSA Research Laboratories, ITS
ESSA Tech. Memorandum ERLTM-ITS 250
Sept. 1970, 12 pages

Rock Electrical Characteristics Deduced from Depth Attenuation Rates (in Drill Holes)
deBettencourt, J. T. and J. W. Frazier
IEEE Trans. Antennas & Propagation
May 1963, Vol. AP-11, No. 3, 358-363

Review of Radio Propagation Below the Earth's Surface
deBettencourt, Joseph T.
URSI Progress in Radio Science, 1963-1966
June 1966, 37 pages

Radio Loss of Lateral Waves in Forest Environments
Dence, D. and T. Tamir
Radio Science
Apr. 1969, Vol. 4, No. 4, 307-318

Air-to-Undersea Communication with Electric Dipoles
Durrani, S. H.
IRE Trans. Antennas & Propagation
Sept. 1962, Vol. AP-10, 524-528

A Study of the Scattering Properties of Inclusions in a Lossy Half-Space
Elliott, R. S. and J. J. Gustincic
U. of CA, School of Engineering & Applied Science
Final Report 69-36, for Dept. Army DA-44-009-AMC-145(T)
Oct. 1969, 154 pages

Submerged Antenna Characteristics
Fenwick, R. C. and W. L. Weeks
IEEE Trans. Antennas & Propagation
May 1963, Vol. AP-11, No. 3, 276-305

Buried Vertically Polarized UHF Antennas
FitzGerrell, R. G., R. L. Gallawa, L. L. Haidle,
A. Q. Howard, Jr., and J. E. Partch
U.S. Office of Telecommunications, ITS
Research Report OT/ITSRR 8
Nov. 1970, 115 pages

Measured Performance of UHF Antennas in Concrete
FitzGerrell, R. G. and L. L. Haidle
U.S. Office of Telecommunications, ITS
Research & Engineering Report 17, OT/TRER 17
Sept. 1971, 145 pages

SAMSO Antenna Measurements: Boeing Prototype Annular Slot
FitzGerrell, R. G.
U.S. Office of Telecommunications, ITS
Apr. 1972, 32 pages

The Radiator-to-Medium Coupling in an Underground Communication System
Ghose, Rabindra Nath
Proc. National Electronics Conference
Oct. 1960, Vol. 16, 279-289

Radiation and Reception with Buried and Submerged Antennas
Hansen, R. C.
IEEE Trans. Antennas & Propagation
May 1963, Vol. AP-11, No. 3, 207-216

The Near Fields of Subsurface Magnetic Dipole Antennas
Hart, William C. and Peter R. Bannister
U.S. Navy Underwater Sound Laboratory
USL Report No. 729
Mar. 7, 1966, 10 pages

UHF Buried Antenna Path Loss Measurements
Hause, L. G. and F. G. Kimmett
U.S. ESSA Research Laboratories, ITS
ESSA Tech. Memorandum ERLTM-ITS 206
Oct. 1969, 53 pages

UHF Radio Propagation Data for Low Antenna Heights, Vol. 1
Hause, L. G., F. G. Kimmett and J. M. Harman
U.S. ESSA Research Laboratories, ITS
ESSA Tech. Report ERL 134-ITS 93-1
Nov. 1969, 1-145

UHF Radio Propagation Data for Low Antenna Heights, Vol. II
Hause, L. G., F. G. Kimmett and J. M. Harman
U.S. ESSA Research Laboratories, ITS
ESSA Tech. Report ERL 134-ITS 93-2
Nov. 1969, 146-341

The Effects of the Air-Earth Interface on the Propagation Constants of a Buried Insulated Conductor
Head, James H.
Naval Electronic Systems Command, Sanguine Div.
[Kaman Nuclear, KN-785-70-6(R)]
Feb. 19, 1970, 39 pages

Propagation Constants of an Insulated Conductor Buried in a Stratified Medium: The Air-Earth and Soil-Rock Interfaces
Head, James H.
Naval Electronic Systems Command, Sanguine Div.
[Kaman Nuclear, KN-785-70-38(R)]
June 1, 1970, 20 pages

Tropical Propagation Research (U), Final Report, Vol. II
Hicks, John J., A. Page Murphy, E. L. Patrick and L. G. Sturgill
U.S. Army Electronics Command
Contract No. DA 36-039 SC-90889, ARPA Order 371
(Atlantic Research)
Nov. 1969, 241 pages

UHF Propagation from Buried Antennas
Hufford, George A.
U.S. ESSA Research Laboratories, ITS
ESSA Tech. Memorandum ERLTM-ITS 191
July 1969, 68 pages

An Experimental Study of the Insulated Dipole Antenna Immersed in a Conducting Medium
Iizuka, Keigo
IEEE Trans. Antennas & Propagation
Sept. 1963, Vol. AP-11, No. 5, 518-532

Dipoles in Dissipative Media
King, Ronold W. P.
"Electromagnetic Waves" - Proceedings of Mathematical Research Center, U.S. Army, Symposium at U. Wisconsin (Apr. 10-12, 1961)
1962, 199-241

The Complete Electromagnetic Field of a Half-Wave Dipole in a Dissipative Medium
King, R. W. P. and K. Iizuka
IEEE Trans. Antennas & Propagation
May 1963, Vol. AP-11, No. 3, 275-285

A Very-Low-Frequency Antenna for Investigating the Ionosphere with Horizontally Polarized Radio Waves
Macmillan, R. S., W. V. T. Rusch and R. M. Golden
NBS J. Research
Jan.-Feb. 1960, Vol. 64D, No. 1, 27-35

A Method for the Measurement of the Parameters of a Two-Layer Stratified Earth
Maley, S. W.
IEEE Trans. Antennas & Propagation
May 1963, Vol. AP-11, No. 3, 366-369

Measured Patterns of HF Antennas and Correlation with Surrounding Terrain
McCoy, D. R., R. D. Wengenroth and J. J. Simons
1969 Conference on Environmental Effects on Antenna Performance Proceedings, Vol. II (J. R. Wait, Editor)
July 14-18, 1969, 28-31

Dipole Radiation in a Conducting Half Space
Moore, R. K. and W. E. Blair
NBS J. Research
Nov.-Dec. 1961, Vol. 65D, No. 6, 547-563

Effects of a Surrounding Conducting Medium on Antenna Analysis
Moore, Richard K.
IEEE Trans. Antennas & Propagation
May 1963, Vol. AP-11, No. 3, 216-225

Generalization of the Concept of Antenna Gain to the Case of Conducting Media
Murav'yev, Yu. K.
Radio Engineering
Jan. 1962, Part 2, Vol. 17, No. 8, 19-22

Lossy Media Propagation at 50 kHz
Murphy, Kenneth and Kurt Ikrath
U.S. Army Electronics Command
Research & Development Tech. Report ECOM-3458
July 1971, 14 pages

Effect of a Finite Conical Plasma Sheath on the Radiation Field of a Dipole
Pridmore-Brown, D. C.
U.S. Air Force Systems Command, AF 04(695)-469
Report No. TDR-469(5220-10)-4, SSD-TDR-64-79
June 21, 1965, 52 pages

Degradation in the Performance of Antennas for Seismic Sensors Caused by the Presence of Snow
Schnetzer, George H.
U.S. AEC by Sandia Laboratories
Development Report SC-DR-71 0486
Sept. 1971, 29 pages

A Study of Arrays of Dipoles in a Semi-Infinite Dissipative Medium
Sivaprasad, K. and R. W. P. King
IEEE Trans. Antennas & Propagation
May 1963, Vol. AP-11, No. 3, 240-256

Nature and Optimisation of the Ground (Lateral) Wave Excited by Submerged Antennas
Staiman, D. and T. Tamir
Proceedings IEE
Aug. 1966, Vol. 113, No. 8, 1299-1310

On the Electromagnetic Field Radiated Above the Tree Tops by an Antenna Located in a Forest
Tamir, T.
U.S. Army Electronics Command
Research & Development Tech. Report ECOM-3443
June 1971, 23 pages

Subsurface Radio Transmission Tests in Cheyenne Mountain
Tsao, Carson K. H.
Air Force Cambridge Research Laboratories
(Prepared by Raytheon Co., Norwood, MA, Contract No. AF19(628)-2362, Project No. 4600, Task No. 460008)
Scientific Report No. 7
Mar. 1965, 31 pages

The Fields of an Electric Dipole in a Semi-Infinite Conducting Medium
Wait, James R. and L. Lorne Campbell
J. Geophysical Research
Mar. 1953, Vol. 58, No. 1, 21-28

Shielding of a Transient Electromagnetic Dipole Field by a Conductive Sheet
Wait, James R.
Canadian J. Physics
Aug. 1956, Vol. 34, No. 8, 890-893

Transmission and Reflection of Electromagnetic Waves in the Presence of Stratified Media
Wait, James R.
NBS J. Research
Sept. 1958 (R.P. 2899), Vol. 61, No. 3, 205-232

Radiation from a Small Loop Immersed in a Semi-Infinite Conducting Medium
Wait, James R.
Canadian J. Physics
May 1959, Vol. 37, No. 5, 672-674

Terrestrial Propagation of Very-Low-Frequency Radio Waves A Theoretical Investigation
Wait, James R.
NBS J. Research
Mar.-Apr. 1960, Vol. 64D, No. 2, 153-204

The Electromagnetic Fields of a Horizontal Dipole in the Presence of a Conducting Half-Space
Wait, James R.
Canadian J. Physics
July 1961, Vol. 39, No. 7, 1017-1028

The Possibility of Guided Electromagnetic Waves in the Earth's Crust
Wait, James R.
IEEE Trans. Antennas & Propagation
May 1963, Vol. AP-11, No. 3, 330-335

Electromagnetic Fields in Lossy Media
Wait, James R.
NBS J. Research
Apr. 1964, Vol. 68D, No. 4, 463-465